Predictive control of field sprayer liquid system

Electronic Systems
Master Thesis
Søren Lang (ES-1025)
Aalborg University
Spring 2024

AALBORG UNIVERSITY

The Technical Faculty of IT and Design
Study board of Electronics and IT
Frederik Bajers Vej 7
9220 Aalborg Øst
http://www.es.aau.dk

Title:
Predictive control of field sprayer liquid system

Project:
P10: Master Thesis
(30 ECTS)

Project period:
February 2024 - May 2024

Project group:
ES-1025

Authors:
Søren Lang (20193480)

Supervisor:
John J. Leth

External company collaboration
Hardi International A/S

Number of pages: 54
Appendix: Page 47 to page 54
Finished: May 2024

Abstract:

Field sprayers are widely used in the agricultural industry to combat weeds and diseases, as well as fertilizing fields. The sprayers perform this task by pumping liquid from a tank through a set of nozzles mounted on a boom and onto the plants on the field. Modern sprayers can automatically turn sets of nozzles on and off based on their location, reducing chemical usage and preventing overlap. Turning the nozzles on or off creates disturbances in the fluid pressure at the boom. It was attempted to use a model predictive controller to control the pressure on the boom, and using its predictive properties to anticipate the impact of the disturbances. Both the use of a nonlinear and a linear controller was investigated, using a nonlinear state space model and a timevariant linear state space model respectively. The nonlinear controller was discarded due to its long execution time. The linear controller was able to fulfill requirements set out by the ISO 16119-2 standard in simulations, and thus moved on to be tested on a test rig emulating a field sprayer. The linear controller was not able to fulfill the requirements set out by the standard when used on the test rig, due to assumptions intended to linearize the model.

Preface

This report is written to document the work performed during the last semester of the masters program in electronic systems at Aalborg University. The project is rated at 30 ECTS points, and ran from the beginning of February 2024 to the end of May 2024.

This project was written in collaboration with the sprayer manufacturer Hardi International. A huge thanks goes out to them for providing a workplace, guidance, test equipment, and lunch.

Reading instructions

Citations in the report are marked with numbers in square brackets, where the source can be found in chapter *Bibliography*. Dates are in the form of dd/mm/yyyy. Tables, figures, etc. are numbered with regard to the chapters, which means that the first figure in chapter 2 will be numbered 2.1, etc. The author have produced the figures and tables without references. Decimal separators are expressed as full stops, thousand separators are expressed as spaces.

Søren Lang
soeren.lang99@gmail.com

Abstract

Field sprayers are widely used in the agricultural industry to combat weeds and diseases, as well as fertilizing fields. The sprayers perform this task by pumping liquid from a tank through a set of nozzles mounted on a boom and onto the plants on the field. Modern sprayers can automatically turn sets of nozzles on and off based on their location, reducing chemical usage and preventing overlap. Turning the nozzles on or off creates disturbances in the fluid pressure at the boom. It was attempted to use a model predictive controller to control the pressure on the boom, and using its predictive properties to anticipate the impact of the disturbances. Both the use of a nonlinear and a linear controller was investigated, using a nonlinear state space model and a timevariant linear state space model respectively. The nonlinear controller was discarded due to its long execution time. The linear controller was able to fulfill requirements set out by the ISO 16119-2 standard in simulations, and thus moved on to be tested on a test rig emulating a field sprayer. The linear controller was not able to fulfill the requirements set out by the standard when used on the test rig, due to assumptions intended to linearize the model.

Synopse

Marksprøjter anvendes vidt og bredt i landbrugsindustrien til at bekæmpe ukrudt og sygdomme, samt til at gøde marker. Sprøjterne klarer denne opgave ved at pumpe væske fra en tank, gennem et sæt dyser monteret på en bom, og ud på planterne på marken. Moderne sprøjter er i stand til, automatisk, at tænde og slukke for individuelle sæt af dyser afhængigt af sprøjtens placering. Dette reducerer mængden af brugte kemikalier samt forhindrer overlap på marken. Ved at tænde eller slukke for dyserne skabes forstyrrelser i væsketrykket ved bommen. Det blev forsøgt at bruge en model predictive controller til at regulere trykket på bommen og bruge dens forudsigende egenskaber til at forvente påvirkningen fra forstyrrelserne. Både brugen af en ikke-lineær og en lineær regulator blev undersøgt ved at bruge henholdsvis en ikke-lineær tilstands-model og en tidsvarierende lineær tilstands-model. Den ikke-lineære regulator blev kasseret på grund af dens lange afviklingstid. I simuleringer var den lineære regulator i stand til at opfylde kravene i ISO 16119-2 standarden, og blev derfor yderligere testet på en testrig, der har de samme funktionaliteter som en sprøjte. Den lineære regulator var ikke i stand til at opfylde kravene i standarden, når den blev brugt på testriggen.

Contents

Chapter 1 Introduction **1**

Chapter 2 Requirements and test description **5**

Chapter 3 Test rig **7**

Chapter 4 Modeling **11**
4.1 Model validation 20
4.2 Linearization 22

Chapter 5 Controller design **26**
5.1 Nonlinear MPC 26
5.1.1 State estimator 26
5.1.2 Controller 30
5.1.3 Controller validation 31
5.2 Linear MPC 34
5.2.1 Controller 35
5.2.2 Controller validation 37

Chapter 6 Acceptance test **39**
6.1 Discussion of results 40

Chapter 7 Conclusion **42**

Chapter 8 Discussion **43**
8.1 Nonlinear MPC 43
8.2 Parameter estimation 43
8.3 Alternative liquid system 44

Bibliography **46**

Appendix A Modelling of regulator valve **47**

Appendix B Modelling of bypass valve **48**

Appendix C Modelling of section valves **49**

Appendix D Modelling of pump **53**

List of Symbols

$\bar{\dot{G}}_R$	Boom/pump ratio time derivative operating point
α	Pump RPM coefficient
$\bar{G}_R$	Boom/pump ratio operating point
$\bar{Q}_p$	Pump flow operating point
$\bar{R}_{pv}$	Equivalent restriction value for sections and bypass operating point
$\bar{\dot{R}}_{pv}$	Equivalent restriction value for sections and bypass time derivative operating point
β	Pump flow coefficient
δ	Pump flow RPM coefficient
Δp	Pressure differential across restriction
Δp_p	Pump pressure differential
ϵ	Pump affine coefficient
γ	Pump second order flow coefficient
$\hat{G}_R$	Boom/pump ratio linearized variable
$\hat{R}_{pv}$	Equivalent restriction value for sections and bypass linearized variable
$\hat{x}$	Estimated state vector
$\hat{x}_{k-1}$	Predicted state space vector from previous time update
$\hat{y}$	Predicted output of plant from previous time update
$\hat{\dot{G}}_R$	Boom/pump ratio time derivative linearized variable
$\hat{\dot{p}}_b$	Linearized boom pressure time derivative
$\hat{\dot{R}}_{pv}$	Equivalent restriction value for sections and bypass time derivative linearized variable
λ	Pump pressure numerator
ω	Pump rotational velocity
ϕ	Zero compensation constant
τ_{G_R}	Boom/pump ratio time constant

τ_{reg}	Regulator valve time constant
τ_{sec}	Section valve time constant
θ_{bp}	Bypass valve opening degree
θ_{reg}	Regulator valve angle
θ_{sec}	Sum of section valve opening degrees
$\tilde{x}_{k-1}$	Predicted state error
$\tilde{y}_{k-1}$	Predicted output error
ε	Model Predictive Controller slack variable
A	State space state matrix
a_{reg}	Regulator valve second order coefficient
B	State space input matrix
B_d	State space disturbance matrix
b_{reg}	Regulator valve first order coefficient
C	State space output matrix
c_{reg}	Regulator valve zeroth order coefficient
F	Discrete time state space function
f	Continuous time state space function
G	Discrete time state space output function
g	Continuous time state space output function
G_{bp}	Bypass valve restriction function gain
G_R	Boom/Pump squared flow ratio
G_{sec}	Section valve restriction function gain
J	Model Predictive Controller cost function
K	Kalman gain
N_c	Model Predictive Controller control horizon
N_p	Model Predictive Controller prediction horizon
P	State error covariance
p_b	Boom pressure
P_{k-1}	Predicted state error covariance from previous time update

Q	Flow through restriction
q	Reference deviation cost multiplier
Q_b	Boom flow
Q_n	State noise covariance
Q_r	Flow through regulator valve
Q_p	Flow from pump
R	Restriction value
r	Setpoint reference for Model Predictive Controller
R_α	Equivalent pump system restriction
R_n	Model output noise covariance
R_p	Constant pump restriction from pump to regulator valve
R_r	Regulator valve time varying restriction
R_{bp}	Restriction of bypass valve and pipe element
R_B	Constant boom restriction from regulator valve to boom sections
R_{eq}	Total boom restriction
R_{pv}	Equivalent restriction value for sections and bypass
R_{sec}	Restriction of currently open boom sections
s	Control signal rate of change cost multiplier
t_s	State estimator sampling time
u	State space input vector
u_d	State space disturbance vector
u_{bp}	Bypass valve control signal
u_{sec}	Section valve control signal
v	Model output noise
v	Slack variable cost multiplier
w	Model state noise
x	State vector
y	Measured plant output
y_{max}	Model Predictive Controller maximum output constraint

$\mathcal{F}$ Lifted MPC state propagation matrix

$\mathcal{Y}$ Stacked MPC predicted output vector

A_a Augmented system state matrix

B_a Augmented system input matrix

$B_{d,a}$ Augmented system disturbance matrix

C_a Augmented system output matrix

$G_{R,max}$ Boom/pump flow ratio maximum value

$G_{R,min}$ Boom/pump flow ratio minimum value

L Lifted MPC input matrix

M Lifted MPC disturbance matrix

1 Introduction

Modern farming uses a lot of different types of equipment, amongst these are field sprayers. Field sprayers are used to apply herbicides, pesticides, fungicides, or fertilizers, collectively referred to as chemicals, to crops. The chemicals are mixed with water and applied to the crops using the sprayer liquid system. Sprayers are maneuverable objects, being moved either by themselves, so-called self-propelled sprayers, or by tractors, as either lift-mounted or trailed sprayers.

Figure 1.1. A trailer sprayer.

A sprayers liquid system consists of three main components: A pump, the boom liquid system, and a liquid control system.

The pump is used to provide pressure and flow for the liquid system. The pump is usually driven by the power take-off (PTO) of the tractor, or in the case of a self-propelled sprayer, by the engine itself. Thus, in these cases, the pump is not controlled by the sprayer.

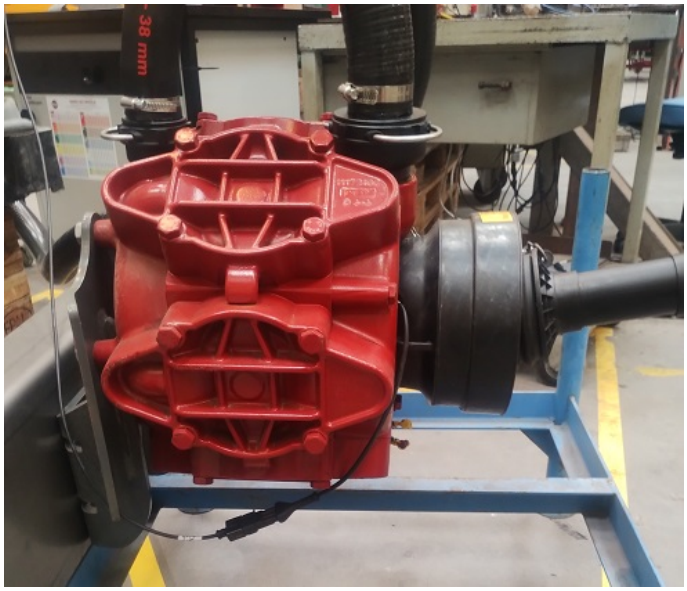

Figure 1.2. A field sprayer pump.

The boom liquid system is the part of the sprayer which applies the chemicals onto the plants. The boom is a metal construction which at Hardi ranges from 15.0 m to 44.0 m. The nozzles on the boom are split into sections, each containing a number of nozzles and is controlled by a section valves. The section valves are binary valves, either letting liquid flow to its nozzles or not.

Figure 1.3. Picture of 3 section valves.

Figure 1.4. Picture of a boom section.

The liquid control system is responsible for controlling the flow to, and the pressure at, the boom, such that the correct amount of water is applied to the field per area. The amount of water applied per area is called the application rate and is a function of how fast the sprayer is going, the width of the boom, and the flow of liquid to the boom. The two main objectives of the liquid control system on modern sprayers are to reduce the amount of chemicals used in the spraying process and to maintain a consistent boom pressure. A reduction in the amount of chemicals used can be accomplished by turning off sections of the sprayer when it moves across areas that do not need to be sprayed, so-called precision spraying, illustrated in figure 1.5. Such systems are already

implemented on several sprayers by a variety of manufacturers, using Global Navigation Satellite Systems (GNSSs) to get the position of the sprayer, and relying on classical control systems for control. Turning sections on or off results in pressure changes in the liquid system, interfering with the flow to the remaining sections. Current control systems use open loop control to prime the system for changing boom conditions.

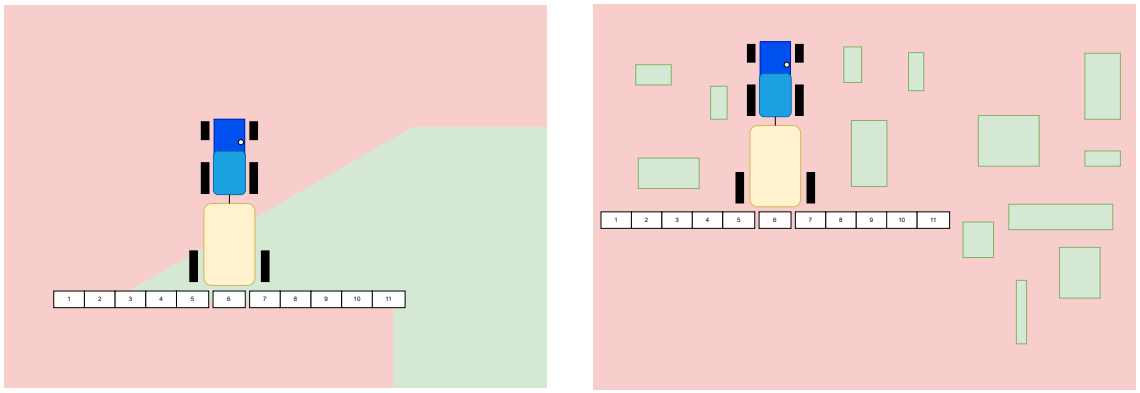

(a) Full field spraying. ***(b)*** Spot spraying.

Figure 1.5. Illustration of precision spraying, green is to be sprayed, red is already sprayed or is not to be sprayed.

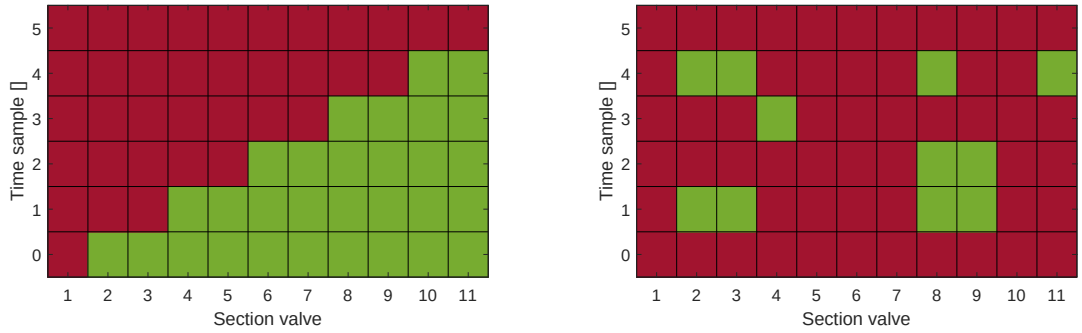

(a) Section spraying. ***(b)*** Spot spraying.

Figure 1.6. Illustration of which sections are on or off in figure 1.5. Green is on, red is off.

Model predictive control (MPC) is a control scheme using a known model to find a series of future control signals which optimizes some defined cost function. A model predictive controller (MPC) can prepare the liquid system for future events, such as switching section valves, if these can be predicted. As the agricultural sector automates a greater and greater deal of work, with more reliable sensors and systems, more and more reliable estimates of the position of the sprayer will become available. This thesis thus proposes that it is possible for an model predictive controller (MPC) to reduce the pressure spikes in the liquid system of field sprayers with sections opening and closing, if the behaviour of the sections can be estimated.

model predictive control has already been considered for controlling the liquid systems on sprayers, such as the work done by Khan et al. [1], Schutz et al. [2], and Felizardo et al. [3], non using the switching sections instead considering these as disturbances.

Khan et al. implemented an MPC onto a sprayer mock up, though their system took the switching for granted and had these as unmeasured disturbances. They did not consider a system where a variable pressure could be present, using a linear model fitted to a single operating point. Their results, when comparing the MPC to a proportional-integral-derivative (PID)-controller, were not impressive, with their MPC resulting in greater pressure spikes and greater rise times.

Schutz et al. looked into using fuzzy logic and predictive control on sprayers where the actuator has dead zones. The fuzzy controller was able to achieve better performance than a PID-controller on several parameters such as overshoot, settling time, all while reducing the wear of the actuators. The article does not deal with a system where the sections are switching, only testing for changes in flow setpoints.

Felizardo et al. used an MPC to control a spray system with a variable application rate. A nonlinear model of the sprayer was developed and linearized online for control purposes. Tests of the controller was performed on a sprayer mockup, and resulted in a performance which was within the limits set by the authors.

The next chapter will delve further into the spraying system used for this thesis, explaining its design, construction, and behavior.

Requirements and test description

2

This chapter will describe requirements for a liquid control system, the requirements will be used in the design of the controller. In the end of the chapter it is described how each requirement will be tested and what the success criteria is.

Requirements for a liquid control system are imposed both by standards, and by the construction of the sprayers themselves. The standard: ISO 16119-2 specifies environmental requirements for sprayers, including the liquid control system [4]. These requirements specify settling time, maximum setpoint offset, and steady state error.

From the standard the following requirements are found:

1. In case of a disturbance, the controller should drive the pressure to within $\pm 7.5\,\%$ of the setpoint
2. The settling time of the application rate should be at most $7.0\,\mathrm{s}$ to within $\pm 10.0\,\%$ when a new application rate setpoint is set
3. At constant pump rotations, constant sprayer velocity, and with no disturbances, the maximum deviation from the mean application rate should not be more than $5.0\,\%$

From the sprayers, the following requirements are found:

A The boom pressure should not exceed $8.0\,\mathrm{bar}$

To verify that the controller can uphold the requirements, the controller will simulate spraying a slice of a field. While running, sections will open and close according to a predefined spray map of the field, shown in figure 2.1. The first $180.0\,\mathrm{m}$ the application rate setpoint will be $300.0\,\mathrm{L\,ha^{-1}}$, afterwards the setpoint will be $200.0\,\mathrm{L\,ha^{-1}}$.

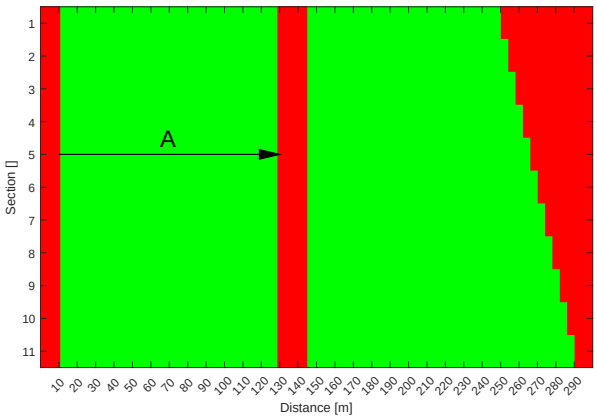

Figure 2.1. Spray map used for testing the controller.

The controller is found to comply with requirement 1 if the pressure falls within the specified range when the section and bypass valves are at steady state along stretch A on the spray map. Requirement 2 is likewise found to be satisfied if the application rate settles within the specified amount of time on stretch A.

Requirement 3 is found to be satisfied if the application does not deviate more than specified on stretch A.

Requirement A is tested by measuring the pressure and checking whether it exceeds the 8.0 bar defined by the requirement.

Four requirements were found which constrains the control systems performance. The requirements puts constraints on the pressure and the application rate. In the next chapter, a test rig is described. The test rig will be used to test the controller, and compare its performance to the requirements.

Test rig 3

This chapter will describe the test rig, which imitates a sprayer, and what components are on it. The test rig will be used to test whether the requirements are satisfied. In the end of the chapter, a block diagram of the control system and the test rig is presented in order to connect all the components in the project.

The test rig used for this thesis is made to represent the liquid system of a sprayer. The system consists of: A water tank, a pump, a fluid regulator valve, a series of section valves, a bypass valve, and a Smartcom electronic control unit (ECU). Figure 3.1 shows the test rig, while figure 3.2 shows where the components would be on a sprayer.

(a) Pump and tank.

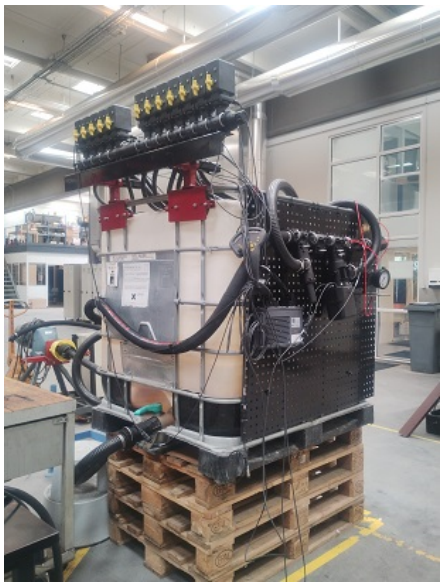

(b) Tank, regulator valve, section valves and bypass valve.

Figure 3.1. Pictures of the sprayer system test rig.

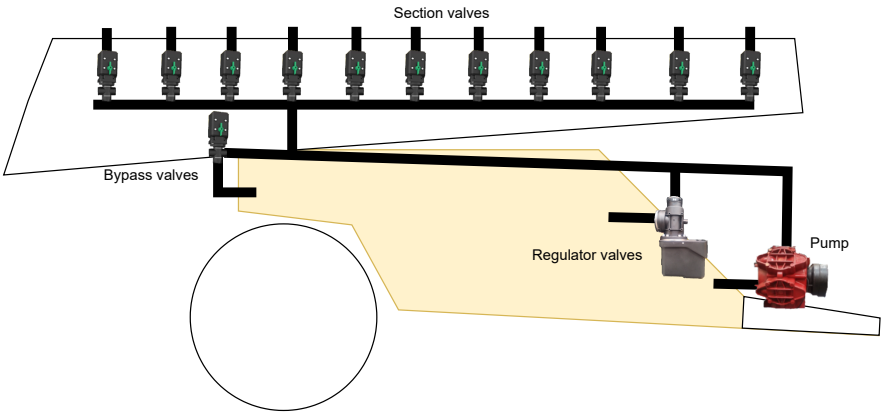

Figure 3.2. Test rig components marked on a sprayer.

Figure 3.3 shows a piping and instrumentation diagram of the system.

The section valves are the actuators providing the primary disturbances to the liquid system. In this project, these will be controlled by a section control system simulating a tractor moving across a field. Each section valve allows liquid to flow to a particular set of nozzles, for simplicity these are placed inside the water tank of the test rig. The pressure inside the tank is usually considered to be at atmospheric pressure, thus the placement of the nozzles have no influence on their pressure characteristic.

The bypass valve allows the water to bypass the boom when none of the section valves are open. The bypass valve is of the same type as the section valves, except it leads the water back to the tank, and thus has no associated nozzles. The bypass valve allows the water coming from the pump to keep circulating and not let the pressure build up.

The regulator valve is the main actuator used by the control system in the current system, it is capable of redirecting parts of the flow from the pump back to the tank, thus reducing the flow to the boom. A controller to move the regulator valve will not be made or described in this thesis, as the main point is to reduce the pressure spikes in the system. A previously made controller for valve movement will be used in the project. This is the only controllable input available for the model predictive controller (MPC), as the control signal for the section valves and bypass valve will be determined by a separate script.

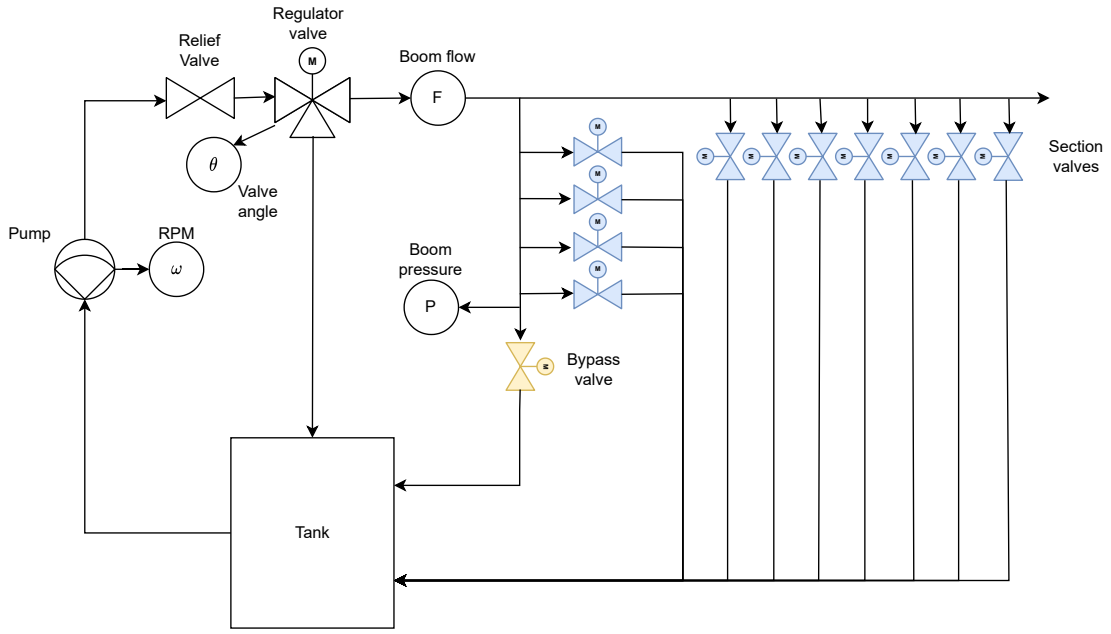

Figure 3.3. Setup of the liquid system.

The pump is not the main actuator for this system due to its interface with the tractor. Usually the pump is driven by the tractors power take-off (PTO) system, resulting in the rotational speed of the pump being proportional to the rotational speed of the motor on the tractor. Some pumps have begun to use hydraulic motors, allowing for changing the revolutions of the pump using a simple valve on the hydraulic lines. This is not the case on the test rig. The test rig will feature a single pump, though some sprayers are equipped with multiple. The addition of an extra pump is not required to show how well model predictive controls (MPCs) perform on sprayer systems.

To prevent the pressure from getting too high for the piping to handle, a relief valve is placed before the regulator valve. The relief valve prevents the pressure from exceeding 8.3 bar.

The system contains four sensors: A flow sensor, a pressure sensor, a regulator valve angle sensor, and a pump revolution sensor. The flow and pressure sensor is used to measure the flow and pressure at the boom. These properties can be used to find the current application rate of the system, for which chapter 2 has several requirements. On current sprayers the two sensors are also used to provide online estimation of the fluid restriction of the boom. The regulator valve angle sensor measures the current opening degree of the regulator valve, and is used primarily to drive the valve to a desired position by an inner loop controller. The pump revolution sensor measures the rotational speed of the pump. The performance of the pump is described partially by its revolutions.

A Hardi Smartcom ECU will be used as an input-output interface for the system. The Smartcom will read the sensor values, actuate the section valves, the bypass valve, and the regulator valve. The setting of each section valve will be determined by a script running on an external PC, communicating with the Smartcom unit via an ISO-canbus connection. The MPC will be implemented on the same PC, generating control signals

for the regulator valve. The smartcom runs on an internal update cycle of 20.0 ms. The proposed control structure of the entire system with the smartcom and the PC is shown in figure 3.4.

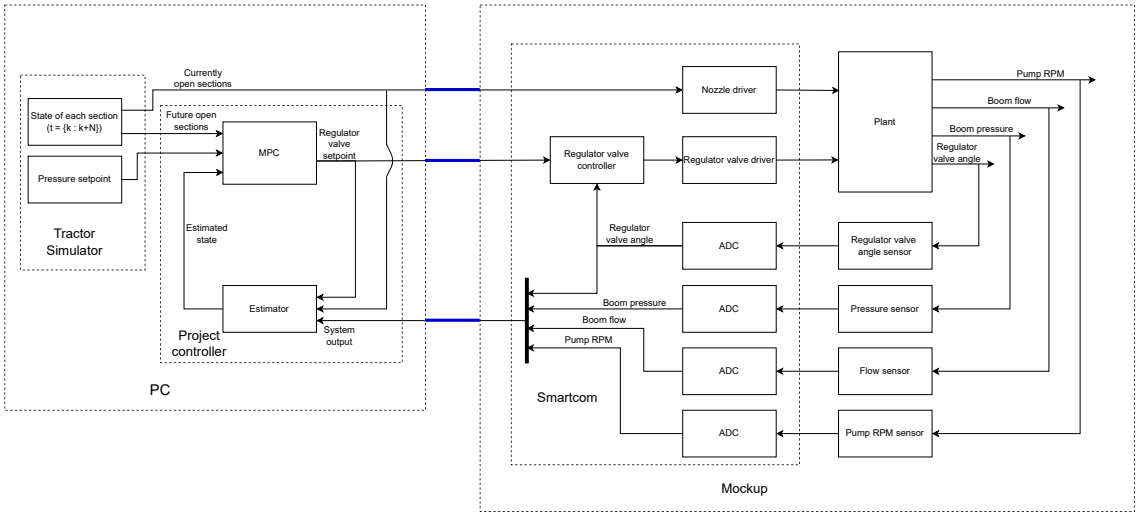

Figure 3.4. Illustration of the proposed controller design.

The purpose of the tractor simulator is to simulate the tractor moving, and a Global Navigation Satellite System (GNSS). The tractor simulator will provide a pressure setpoint for the controller based upon an application rate setpoint. To obtain the application rate setpoint, the simulator will assume a boom width of 24.0 m and a driving speed of 20.0 km h^{-1}. The tractor simulator will include an algorithm that will decide which section and bypass valves are open, this will be referred to as the auto section controller (ASC). The ASC will provide a list of which section valves are open some update cycles into the future.

This chapter described the test rig and its components: The pump, regulator valve, bypass valve, section valve, the ECU, and the sensors. The relationship between the test rig and the proposed controller was established. Supporting systems for the controller was introduced, the systems will be used in order to emulate the parts of the spraying process which the test rig is not capable of, e.g. the tractor, the GNSS-system, and the ASC. The next chapter will develop a model of the test rig, and in extension a sprayer.

Modeling 4

This chapter will deal with modelling the test rig described in chapter 3, it is made to emulate the liquid system of a sprayer when operating in the field. The models will derive dynamic models describing the boom pressure. The models resulting from the chapter will be used for the model predictive controllers (MPCs) in the next chapter.

A liquid diagram of the test rig is shown in figure 4.1. The regulator valve is modelled as a variable restriction, likewise, the sections and their valves are modelled as a combined variable restriction. The section valve restriction are defined to be very large when the valves are closed, and the combined restriction of the nozzles when open. The bypass valve is modelled in a similar manner.

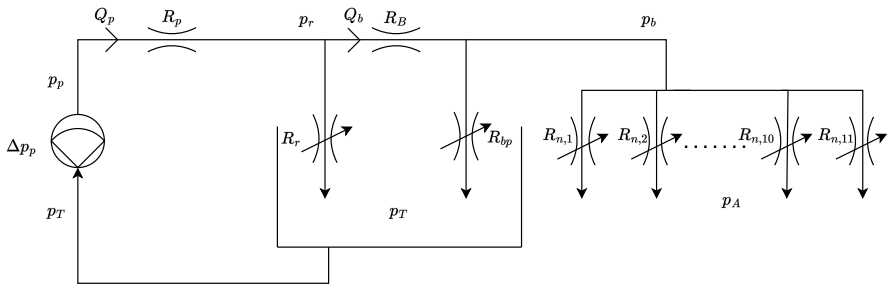

Figure 4.1. Fluid diagram of the spraying system.

To simplify the system, the assumptions below are made. From the assumptions, a simplified liquid diagram is presented in figure 4.2.

1. All sections contain the same amount of nozzles and the same type of nozzles
2. The tank is at atmospheric pressure: $p_T = p_A$
3. The section valves can all be described by a single function R_{sec}
4. The flow into the pump is the same as the instantaneous flow out of the pump
5. The rotational speed of the pump is constant

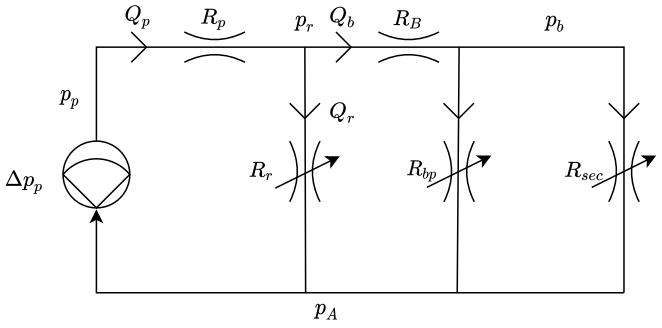

Figure 4.2. Simplified fluid diagram of figure 4.1 using the defined assumptions.

The system will be modelled using the hydraulic equivalent of Kirchhoffs current and voltage laws [5]. Each element in the system will have an associated pressure drop from one end to the other, a pressure differential. The pressure drop is going to be given as a function of the flow through the element and the restriction of the element [6]. Summing the pressure differentials in any loop throughout the system, with their associated sign, will result in a pressure drop of 0, thus the pressure is equivalent to the voltage in the analogy of Kirchhoffs laws. As for Kirchhoffs current law, the flow in and out of any node in the system will sum to 0 when considering their respective sign.

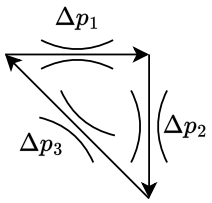

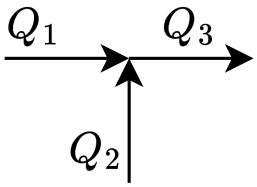

$$\Delta p_1 + \Delta p_2 + \Delta p_3 = 0 \qquad Q_1 + Q_2 - Q_3 = 0$$

The dynamic models in this chapter will be based upon time derivatives of steady state equations for the system. Dynamic pipe models derived via control volume approaches will not be considered in this thesis, as the resulting fast dynamics combined with the relative slow dynamics of the valves, results in a stiff system model. Additionally, from tests on the test rig, the dominant dynamics originate from the valves in the system.

The steady state pressure drop over a restriction R is given by equation 4.1. As the flow in the system is only meant to move in the directions marked on figure 4.2, the flow term Q^2 is used instead of the more generic term $|Q|Q$.

$$\Delta p = R\, Q^2 \tag{4.1}$$

Δp	Pressure differential across restriction	[bar]
Q	Flow through restriction	$[\mathrm{L\,min^{-1}}]$
R	Restriction value	$[\mathrm{min^2\,L^{-2}}]$

Pumps are complex but is in this case modelled as pressure sources, providing a pressure differential as a function of the flow through the pump and the rotational velocity of the pump.

$$\Delta p_p = p_p(Q, \omega) \tag{4.2}$$

The boom pressure p_b is the primary variable deciding the effectiveness of the liquid system, as it decides the flow out of each nozzle irrelevant of how many nozzles are open. The pressure is described in equation 4.3 by the boom flow Q_b, and the equivalent restriction R_{pv}, describing the parallel restrictions of the bypass and section valves. This restriction is based on whether the bypass valve is open and how many section valves are open at any given time.

$$\begin{aligned} p_b &= R_{pv}\, Q_b^2 \\ R_{pv} &= \frac{R_{bp}\, R_{sec}}{\left(\sqrt{R_{bp}} + \sqrt{R_{sec}}\right)^2} \end{aligned} \tag{4.3}$$

p_b	Boom pressure	[bar]
Q_b	Boom flow	$[\mathrm{L\,min^{-1}}]$
R_{pv}	Equivalent restriction value for sections and bypass	$[\mathrm{min^2\,L^{-2}}]$
R_{bp}	Restriction of bypass valve and pipe element	$[\mathrm{min^2\,L^{-2}}]$
R_{sec}	Restriction of currently open boom sections	$[\mathrm{min^2\,L^{-2}}]$

Defining, the boom equivalent restriction R_{eq} as the series connection of the constant boom restriction R_B and the valve equivalent restriction R_{pv}, it is possible to simplify the model in figure 4.2 even further into the model in figure 4.3.

$$R_{eq} = \frac{R_{bp}\, R_{sec}}{\left(\sqrt{R_{bp}} + \sqrt{R_{sec}}\right)^2} + R_B = R_{pv} + R_B \tag{4.4}$$

R_{eq}	Total boom restriction	$[\mathrm{min^2\,L^{-2}}]$
R_B	Constant boom restriction from regulator valve to boom sections	$[\mathrm{min^2\,L^{-2}}]$

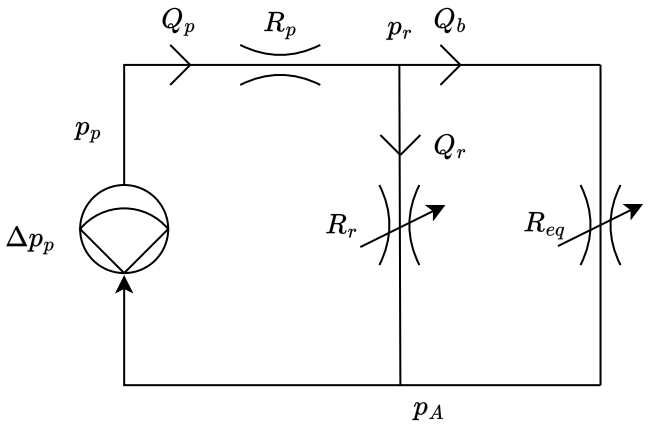

Figure 4.3. Further simplified liquid diagram.

A function describing the two boom restrictions, R_{bp}, R_{sec}, are found in appendices B and C respectively. The bypass valve restriction is defined by its opening degree θ_{bp} which is defined to be in the range [0,1], where 0 is fully closed, and 1 is fully open. The valves function is given in equation 4.5. The zero compensation variable ϕ is added to the function parameter such that the function is defined for $\theta_{bp} = 0$, the value is chosen to be 100.0E−6.

$$R_{bp}(\theta_{bp}) = \frac{G_{bp}}{\theta_{bp} + \phi} \tag{4.5}$$

θ_{bp}	Bypass valve opening degree	$[\cdot]$
G_{bp}	Bypass valve restriction function gain	$[\text{min}^2\,\text{L}^{-2}]$
ϕ	Zero compensation constant	$[\cdot]$

The section valve restriction is given by equation 4.6. The parameter θ_{sec} does not represent the opening degree of a single valve, but instead the combined opening degree of all the section valves, thus for the test rig it is defined in the range [0,11]. A zero compensation term is once again added in order to define the function for $\theta_{sec} = 0$. Due to the function representing a set of parallel restrictions, the control signal, the denominator, is squared.

$$R_{sec}(\theta_{sec}) = \frac{G_{sec}}{(\theta_{sec} + \phi)^2} \tag{4.6}$$

θ_{sec}	Sum of section valve opening degrees	$[\cdot]$
G_{sec}	Section valve restriction function gain	$[\text{min}^2\,\text{L}^{-2}]$

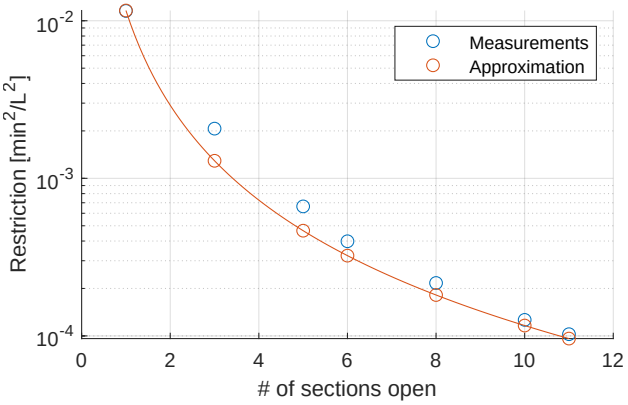

Figure 4.4. Section valve restrictions as a function of number of valves open.

The flow through the regulator valve can be described using the boom flow, as shown in equation 4.7. The resulting regulator flow is thus described merely by the boom flow, the model predictive control (MPC) controlled restriction value R_r, and the section valve controlled restriction R_{eq}.

$$\begin{aligned} Q_r^2 &= \frac{p_r}{R_r} = Q_b^2 \frac{R_{eq}}{R_r} \\ Q_r &= Q_b \sqrt{\frac{R_{eq}}{R_r}} \end{aligned} \tag{4.7}$$

Q_r	Flow through regulator valve	$[\mathrm{L\,min^{-1}}]$
R_r	Regulator valve time varying restriction	$[\mathrm{min^2\,L^{-2}}]$

The regulator valve restriction R_r is defined by a function found in appendix A, shown in equation 4.8. The input θ_{reg} represents how open the valve is, it is defined in the range $[-40, 40]$ and is given in degrees.

$$R_r(\theta_{reg}) = \frac{1}{(a_{reg}\theta_{reg}^2 - b_{reg}\theta_{reg} + c_{reg})^2} \tag{4.8}$$

θ_{reg}	Regulator valve angle	$[\cdot]$
a_{reg}	Regulator valve second order coefficient	$[\mathrm{L\,min^{-1}}]$
b_{reg}	Regulator valve first order coefficient	$[\mathrm{L\,min^{-1}}]$
c_{reg}	Regulator valve zeroth order coefficient	$[\mathrm{L\,min^{-1}}]$

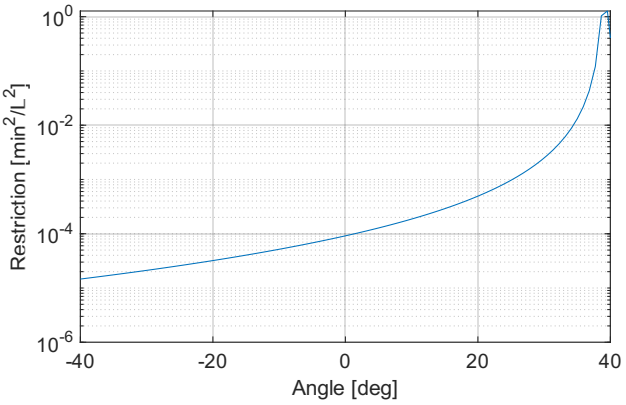

Figure 4.5. Regulator valve restriction as a function of θ_{reg}.

The boom flow is the flow coming from the pump but without the flow going through the regulator valve, $Q_b = Q_p - Q_r$. Q_b can therefore be described by equation 4.9. The equation provides a gain, G_R, describing the relation between the boom flow and the pump flow.

$$\begin{aligned} Q_b &= Q_p - Q_b \sqrt{\frac{R_{eq}}{R_r}} \\ \rightarrow Q_b &= Q_q \frac{\sqrt{R_r}}{\sqrt{R_r} + \sqrt{R_{eq}}} = Q_p \sqrt{G_R} \end{aligned} \tag{4.9}$$

Q_p	Flow from pump	$[\mathrm{L\,min^{-1}}]$
G_R	Boom/Pump squared flow ratio	$[\cdot]$

Equation 4.9 also provides a method for describing the boom pressure using only the pump flow, the regulator valve restriction, and the bypass and section valves restrictions.

$$\begin{aligned} p_b &= R_{pv} Q_b^2 \\ p_b &= R_{pv}\, G_R Q_p^2 \end{aligned} \tag{4.10}$$

For control purposes it is desired to generate a first order differential equation describing $\dot{p}_b$, this is done by differentiating equation 4.10 with respect to time. The non-differential terms Q_p^2 in the equation is given by $Q_p^2 = \frac{p_b}{R_{pv} G_R}$, derived from equation 4.10

$$\begin{aligned} \dot{p}_b &= \frac{d}{dt} p_b \\ &= R_{pv}\, G_R \, \frac{d}{dt} Q_p^2 + G_R Q_p^2 \, \frac{d}{dt} R_{pv} + Q_p^2 R_{pv} \, \frac{d}{dt} G_R \end{aligned} \tag{4.11}$$

The differential $\frac{d}{dt}R_{pv}$ is expanded in equation 4.12.

$$\begin{aligned}
\frac{d}{dt}R_{pv} &= \frac{d}{dt}\frac{R_{bp}R_{sec}}{\left(\sqrt{R_{bp}}+\sqrt{R_{sec}}\right)^2} \\
&= \left(\sqrt{R_{bp}}+\sqrt{R_{sec}}\right)^{-2}\frac{d}{dt}R_{bp}R_{sec} + R_{bp}R_{sec}\frac{d}{dt}\left(\sqrt{R_{bp}}+\sqrt{R_{sec}}\right)^{-2} \\
&= \frac{R_{bp}\dot{R}_{sec}+R_{sec}\dot{R}_{bp}}{\left(\sqrt{R_{bp}}+\sqrt{R_{sec}}\right)^2} - 2\frac{R_{bp}R_{sec}}{\left(\sqrt{R_{bp}}+\sqrt{R_{sec}}\right)^3}\frac{d}{dt}\left(\sqrt{R_{bp}}+\sqrt{R_{sec}}\right) \\
&= \frac{R_{bp}\dot{R}_{sec}+R_{sec}\dot{R}_{bp}}{\left(\sqrt{R_{bp}}+\sqrt{R_{sec}}\right)^2} - 2\frac{R_{bp}R_{sec}}{\left(\sqrt{R_{bp}}+\sqrt{R_{sec}}\right)^3}\frac{d}{dt}\left(\frac{\dot{R}_{bp}}{2\sqrt{R_{bp}}}+\frac{\dot{R}_{sec}}{2\sqrt{R_{sec}}}\right) \\
&= \frac{R_{sec}^{1.5}}{\left(\sqrt{R_{bp}}+\sqrt{R_{sec}}\right)^3}\dot{R}_{bp} + \frac{R_{bp}^{1.5}}{\left(\sqrt{R_{bp}}+\sqrt{R_{sec}}\right)^3}\dot{R}_{sec}
\end{aligned} \tag{4.12}$$

In appendix C it was found that the section valves act as a first order system, illustrated by the step responses in figure 4.6. The the dynamics introduced by the section valves are modelled by having the opening degree θ_{sec} act as the first order ordinary differential equation in 4.13, with the input given by the control signal u_{sec}. The bypass valve is of the same type as the section valves, thus these are described by the same function.

$$\begin{aligned}
\dot{\theta}_{sec} &= \frac{-1}{\tau_{sec}}\theta_{sec} + \frac{1}{\tau_{sec}}u_{sec} \\
\rightarrow \dot{R}_{sec} &= \frac{-2G_{sec}}{(\theta_{sec}+\phi)^3}\dot{\theta}_{sec} \\
\dot{\theta}_{bp} &= \frac{-1}{\tau_{sec}}\theta_{bp} + \frac{1}{\tau_{sec}}u_{bp} \\
\rightarrow \dot{R}_{bp} &= \frac{-G_{bp}}{(\theta_{bp}+\phi)^2}\dot{\theta}_{bp}
\end{aligned} \tag{4.13}$$

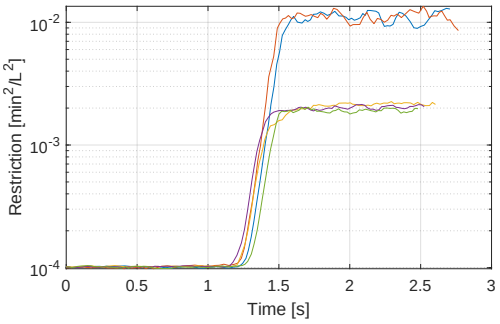

Figure 4.6. Step responses for the section valves.

u_{sec}	Section valve control signal	$[\cdot]$
u_{bp}	Bypass valve control signal	$[\cdot]$
τ_{sec}	Section valve time constant	[s]

The differential term $\frac{d}{dt}G_r$, is derived in equation 4.14. Note that $\dot{R}_{eq} = \dot{R}_{pv}$.

$$\begin{aligned}
\frac{d}{dt}G_r &= \frac{d}{dt}\frac{R_r}{\left(\sqrt{R_r}+\sqrt{R_{eq}}\right)^2} \\
&= R_r\frac{d}{dt}\left(\sqrt{R_r}+\sqrt{R_{eq}}\right)^{-2} + \left(\sqrt{R_r}+\sqrt{R_{eq}}\right)^{-2}\frac{d}{dt}R_r \\
&= \frac{-2R_r}{\left(\sqrt{R_r}+\sqrt{R_{eq}}\right)^3}\frac{d}{dt}\left(\sqrt{R_r}+\sqrt{R_{eq}}\right) + \frac{\dot{R}_r}{\left(\sqrt{R_r}+\sqrt{R_{eq}}\right)^2} \\
&= \frac{\dot{R}_r R_{eq} - R_r\dot{R}_{eq}}{\left(\sqrt{R_r}+\sqrt{R_{eq}}\right)^3\sqrt{R_{eq}}}
\end{aligned} \tag{4.14}$$

For the sake of simplicity, the differential regulator restriction is modelled by having the valve angle θ_{reg} behave as a first order system, given by equation 4.15, in the same manner as the section and bypass valves.

$$\begin{aligned}
\dot{\theta}_{reg} &= \frac{-1}{\tau_{reg}}\theta_{reg} + \frac{1}{\tau_{reg}}u_{reg} \\
\rightarrow \dot{R}_r &= \frac{-2\ (2\ a_{reg}\ \theta_{reg} + b_{reg})}{(a_{reg}\ \theta_{reg}^2 - b_{reg}\ \theta_{reg} + c_{reg})^3}\ \dot{\theta}_{reg}
\end{aligned} \tag{4.15}$$

τ_{reg}	Regulator valve time constant	[s]

The pump is modelled using equation 4.16. The model was chosen from a series of fitted functions, described in appendix A. The model was not the one with the absolutely best fit, it was the second best, though the models behaviour in the operating area was more well behaved.

$$\Delta p_p(Q_p, \omega) = \alpha\ \omega + \beta\ Q_p + \gamma\ Q_p^2 + \delta\ \omega\ Q_p + \epsilon \tag{4.16}$$

Δp_p	Pump pressure differential	[bar]
ω	Pump rotational velocity	[rpm]
α	Pump RPM coefficient	[bar rpm^{-1}]
β	Pump flow coefficient	[bar min L^{-1}]
γ	Pump second order flow coefficient	[bar min^2 L^{-2}]
δ	Pump flow RPM coefficient	[bar min L^{-1} rpm^{-1}]
ϵ	Pump affine coefficient	[bar]

The pressure across the pump can also be described by the restrictions and flows in the remaining parts of the system, as done by equation 4.17.

$$\begin{aligned}\Delta p_p &= R_p Q_p^2 + R_{eq} Q_b^2 \\ &= R_p Q_p^2 + R_{eq} G_R Q_p^2 = R_\alpha Q_p^2\end{aligned} \tag{4.17}$$

R_p	Constant pump restriction from pump to regulator valve	$[\mathrm{min}^2\,\mathrm{L}^{-2}]$
R_α	Equivalent pump system restriction	$[\mathrm{min}^2\,\mathrm{L}^{-2}]$

Equation 4.17 can be combined with equation 4.16 to achieve a model for the pump, where the only time dependent variable is the pump flow.

$$\begin{aligned}R_\alpha Q_p^2 &= \alpha\omega + \beta Q_p + \gamma Q_p^2 + \delta\omega Q_p + \epsilon \\ Q_p &= \frac{\beta + \delta\omega \pm \sqrt{(\beta+\delta\omega)^2 + 4(R_\alpha - \gamma)(\alpha\omega + \epsilon)}}{2(R_\alpha - \gamma)} = \frac{\lambda(R_\alpha,\ \omega)}{2(R_\alpha - \gamma)}\end{aligned} \tag{4.18}$$

λ	Pump pressure numerator	$[\mathrm{L\,min}^{-1}]$

The time derivative for Q_p is given by equation 4.19.

$$\dot{Q}_p = \frac{\pm 2(\alpha\omega + \epsilon)\dot{R}_\alpha}{2(R_\alpha - \gamma)\sqrt{(\beta+\delta\omega)^2 + 4(R_\alpha - \gamma)(\alpha\omega + \epsilon)}} - \frac{2\dot{R}_\alpha\ \lambda}{(2R_\alpha - 2\gamma)^2} \tag{4.19}$$

The final differential term for this model is $\dot{R}_\alpha$, which is derived in equation 4.20.

$$\begin{aligned}\dot{R}_\alpha &= \frac{d}{dt}\left(R_p + R_{eq}\ G_R\right) \\ &= G_R\ \frac{d}{dt}\ R_{eq} + R_{eq}\ \frac{d}{dt}\ G_R = G_R\ \frac{d}{dt}\ R_{pv} + R_{eq}\ \frac{d}{dt}\ G_R \\ &= \frac{\dot{R}_{pv}\ R_r^{1.5} + \dot{R}_r\ R_{eq}^{1.5}}{\left(\sqrt{R_r} + \sqrt{R_{eq}}\right)^3}\end{aligned} \tag{4.20}$$

Putting everything together and including the first order characteristics for R_r, R_{sec} and R_{bp}, results in the set of four ordinary differential equations in equation 4.21. Table 4.1 list the value of the parameters which has been measured and fitted for the model.

$$
\begin{aligned}
\dot{p}_b &= 2\,R_{pv}\,G_R\,\dot{Q}_p + G_R\frac{p_b}{R_{pv}G_R}\,\dot{R}_{pv} + \frac{p_b}{R_{pv}G_R}R_{pv}\,\dot{G}_R \\
\dot{\theta}_{bp} &= -\frac{1}{\tau_{bp}}\theta_{bp} + \frac{1}{\tau_{bp}}u_{bp} \\
\dot{\theta}_{sec} &= -\frac{1}{\tau_{sec}}\theta_{sec} + \frac{1}{\tau_{sec}}u_{sec} \\
\dot{\theta}_{reg} &= -\frac{1}{\tau_{reg}}\theta_{reg} + \frac{1}{\tau_{reg}}u_{reg}
\end{aligned}
\tag{4.21}
$$

Constant	Value
R_B	$99.1\text{E}{-3}\,\text{min}^2\,\text{L}^{-2}$
R_P	$115.0\text{E}{-3}\,\text{min}^2\,\text{L}^{-2}$
a_{reg}	$15.8\text{E}{-3}\,\text{L}\,\text{min}^{-1}$
b_{reg}	$-3.3\,\text{L}\,\text{min}^{-1}$
c_{reg}	$104.6\,\text{L}\,\text{min}^{-1}$
G_{sec}	$11.6\text{E}{-3}\,\text{min}^2\,\text{L}^{-2}$

Constant	Value
τ_{sec}	$152.0\text{E}{-3}\,\text{s}$
G_{bp}	$67.9\text{E}{-6}\,\text{min}^2\,\text{L}^{-2}$
α	$880.0\text{E}{-3}\,\text{bar}\,\text{rpm}^{-1}$
β	$-1.9\,\text{bar}\,\text{min}\,\text{L}^{-1}$
γ	$3.7\text{E}{-3}\,\text{bar}\,\text{min}^2\,\text{L}^{-2}$
δ	$1.7\text{E}{-3}\,\text{bar}\,\text{min}\,\text{L}^{-1}\,\text{rpm}^{-1}$
ϵ	$73.8\,\text{bar}$

Table 4.1. Values for constants in the model.

4.1 Model validation

In this section the model derived is validated by comparing simulations of the model to step responses performed on the test rig. Comparisons will be performed when changing the number of open section valves, when switching to the bypass, and when changing the angle of the regulator valve.

Figure 4.7 shows steps for different setpoints in the amount of open section valves. The model is able to reach the same steady state level as the system, though with some deviation in the rise time. But considering the low root mean squared (RMS)-error of both step responses, this is not considered a problem.

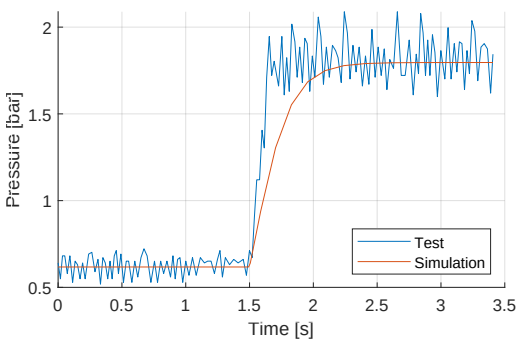

(a) From 11 open sections to 1 open section, RMS-error = 170.0E−3 bar.

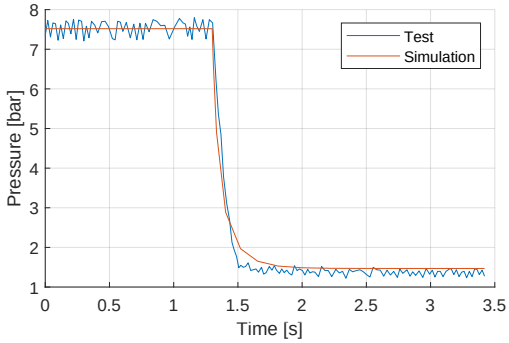

(b) From 1 open section to 11 open sections, RMS-error = 250.0E−3 bar.

Figure 4.7. Step responses for changes in number of open sections.

Figure 4.8 shows step responses for the bypass valve. The significant deviation between the simulation and the measurement in figure 4.8a is due to an over- or underestimation of either the bypass valve restriction or section valve restriction. On a production sprayer a parameter estimator would be present to estimate these in real time, due to the type of nozzles being unknown, and therefore their restrictions. Such an estimator is not made in this project.

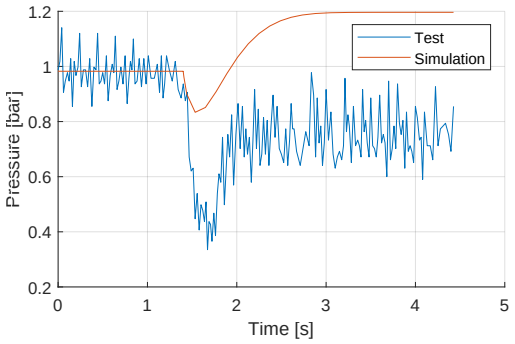

(a) From 0 open sections to 11 open sections, RMS-error = 200.0E−3 bar.

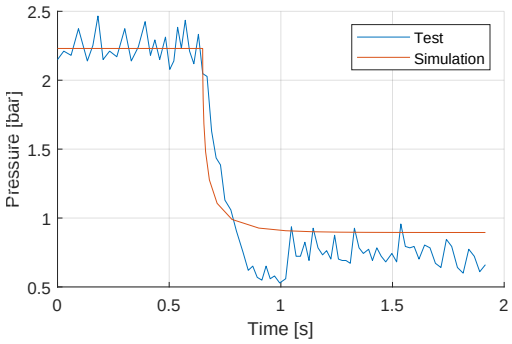

(b) From 5 open sections to 0 open sections, RMS-error = 350.0E−3 bar.

Figure 4.8. Step responses for changes in number of open sections.

Figure 4.9 shows step responses for the regulator valve. This is only done for validation as a first order system does not appropriately describe the regulator valve.

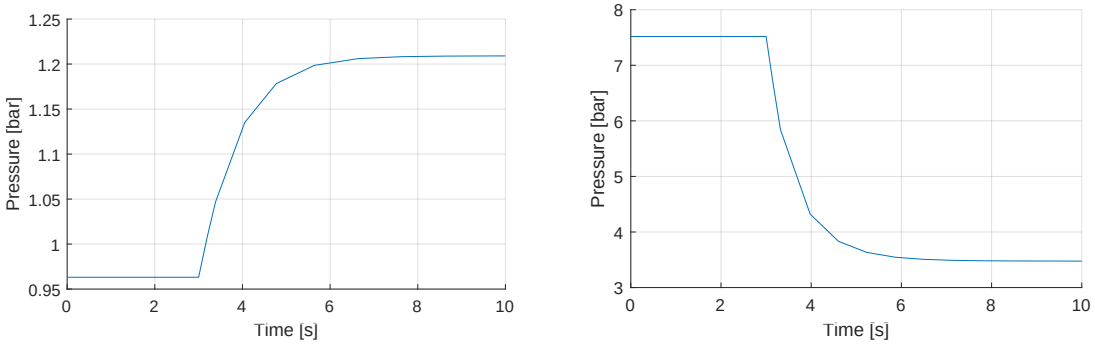

(a) From 3.0 deg to 10.0 deg. ***(b)*** From 12.0 deg to 0.0 deg.

Figure 4.9. Step responses for change in regulator valve angle.

4.2 Linearization

The linearized model is, like the nonlinear model, based on the function describing boom pressure using the pump flow from equation 4.10. An additional assumption is made, however, which results in a linear time variant model. The primary assumption is that, given constant pump rotations, the pump flow, Q_p, is constant and independent of the number of open sections and the position of the regulator valve. This assumption is based upon the pump flow found when doing step responses on the section valves, with the pump flow from some of the tests shown in figure 4.10.

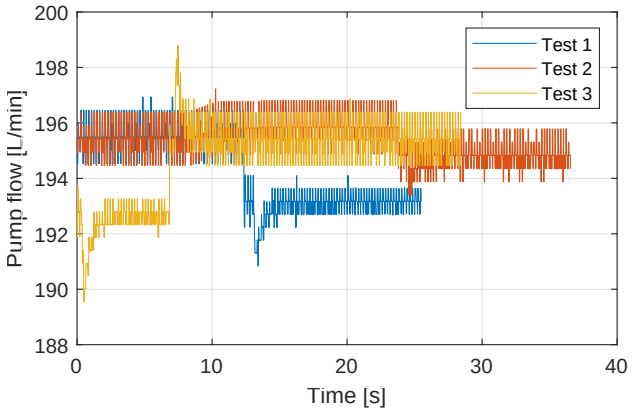

Figure 4.10. Pump flow Q_p while performing step responses on the section valves.

The pump boom gain, G_R, is not expanded in this model, and is used as the control signal. The idea being that a controller would generate a specific gain, and afterwards be translated via a nonlinear function into a position for the regulator valve, the transformation is depicted in figure 4.11. The dynamic description of the model is thus given by equation 4.22.

$$\begin{aligned} p_b &= R_{pv}\, G_R\, \bar{Q}_p^2 \\ \dot{p}_b &= R_{pv}\, \bar{Q}_p^2\, \dot{G}_R + G_R\, \bar{Q}_p^2\, \dot{R}_{pv} \end{aligned} \tag{4.22}$$

$\bar{Q}_p$ | Pump flow operating point $[\mathrm{L\,min^{-1}}]$

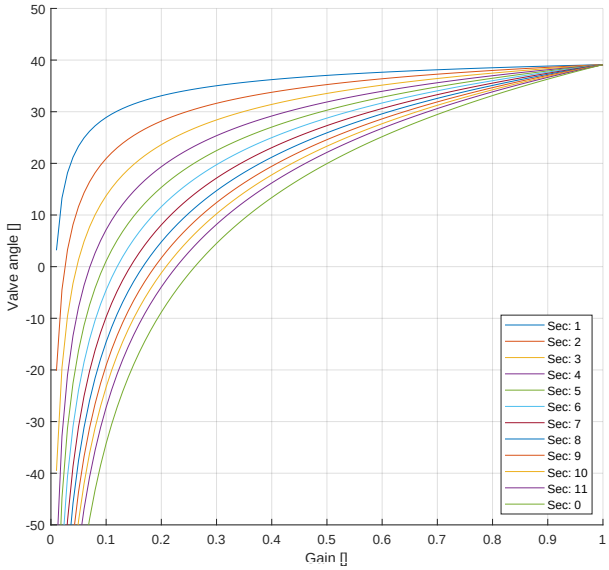

Figure 4.11. Relationship between the gain G_R and the regulator valve angle.

Equation 4.22 is still nonlinear, and therefore it is linearized using a taylor approximation, resulting in equation 4.23.

$$\begin{aligned} \hat{\dot{p}}_b = &\left(\hat{G}_R - \bar{G}_R\right)\, \bar{Q}_p^2\, \bar{\dot{R}}_{pv} + \left(\hat{R}_{pv} - \bar{R}_{pv}\right)\, \bar{Q}_p^2\, \bar{\dot{G}}_R \\ &+ \left(\hat{\dot{G}}_R - \bar{\dot{G}}_R\right)\, \bar{Q}_p^2\, \bar{R}_{pv} + \left(\hat{\dot{R}}_{pv} - \bar{\dot{R}}_{pv}\right)\, \bar{Q}_p^2\, \bar{G}_R \end{aligned} \tag{4.23}$$

$\bar{G}_R$	Boom/pump ratio operating point	$[\cdot]$
$\bar{R}_{pv}$	Equivalent restriction value for sections and bypass operating point	$[\mathrm{min}^2\,\mathrm{L}^{-2}]$
$\bar{\dot{G}}_R$	Boom/pump ratio time derivative operating point	$[\mathrm{s}^{-1}]$
$\bar{\dot{R}}_{pv}$	Equivalent restriction value for sections and bypass time derivative operating point	$[\mathrm{min}^2\,\mathrm{L}^{-2}\,\mathrm{s}^{-1}]$
$\hat{G}_R$	Boom/pump ratio linearized variable	$[\cdot]$
$\hat{R}_{pv}$	Equivalent restriction value for sections and bypass linearized variable	$[\mathrm{min}^2\,\mathrm{L}^{-2}]$
$\hat{\dot{G}}_R$	Boom/pump ratio time derivative linearized variable	$[\mathrm{s}^{-1}]$
$\hat{\dot{R}}_{pv}$	Equivalent restriction value for sections and bypass time derivative linearized variable	$[\mathrm{min}^2\,\mathrm{L}^{-2}\,\mathrm{s}^{-1}]$
$\hat{\dot{p}}_b$	Linearized boom pressure time derivative	$[\mathrm{bar}\,\mathrm{s}^{-1}]$

It is assumed that the operating points $\bar{\dot{R}}_{pv} = \bar{\dot{G}}_R = 0$ as the pressure should be at rest when the system is at steady state. The operating points $\bar{R}_{pv}$ and $\bar{G}_R$ are chosen to be time varying, thus being updated on each controller update. The resulting linearized model is shown in equation 4.24.

$$\hat{\dot{p}}_b = \hat{\dot{G}}_R\ \bar{Q}_p^2\ \bar{R}_{pv} + \hat{\dot{R}}_{pv}\ \bar{Q}_p^2\ \bar{G}_R \tag{4.24}$$

Equation 4.12 is used to describe the term $\hat{\dot{R}}_{pv}$, the differential parts $\dot{R}_{sec}$, and $\dot{R}_{bp}$ will be used as measured disturbances as these are determined by the section controller. The term $\hat{\dot{G}}_R$ will be described by a first order system with a time constant τ_{G_R}.

$$\hat{\dot{R}}_{pv} = G_{bp}(R_{bp},\ R_{sec})\ \dot{R}_{bp} + G_{sec}(R_{bp},\ R_{sec}) \tag{4.25}$$

$$\begin{aligned}\hat{\dot{p}}_b = &\left(\frac{1}{\tau_{G_R}} u_{G_R} - \frac{1}{\tau_{G_R}} G_R\right)\ \bar{Q}_p^2\ \bar{R}_{pv} \\ &+ \left(G_{bp}(r_{bp}, r_{sec})\ \dot{R}_{bp} + G_{sec}(r_{bp}, r_{sec})\dot{R}_{sec}\right)\ \bar{Q}_p^2\ \bar{G}_R\end{aligned} \tag{4.26}$$

The linear model can then be described by the state space matrices in equation 4.27.

$$\begin{aligned} A &= \begin{bmatrix} 0 & -\frac{G_R}{\tau_{G_R}}\bar{Q}_p^2\bar{R}_{pv} \\ 0 & -\frac{1}{\tau_{G_R}} \end{bmatrix} & B &= \begin{bmatrix} \frac{1}{\tau_{G_R}} \\ \frac{1}{\tau_{G_R}} \end{bmatrix} & x &= \begin{bmatrix} p_b \\ G_R \end{bmatrix} & u &= \begin{bmatrix} u_{G_R} \end{bmatrix} \\ B_d &= \begin{bmatrix} G_{bp}\bar{Q}_p^2\bar{G}_R & G_{sec}\bar{Q}_p^2\bar{G}_R \\ 0 & 0 \end{bmatrix} & C &= \begin{bmatrix} 1 & 0 \\ 0 & 1 \end{bmatrix} & u_d &= \begin{bmatrix} \dot{R}_{bp} \\ \dot{R}_{sec} \end{bmatrix} \end{aligned} \tag{4.27}$$

τ_{G_R}	Boom/pump ratio time constant	[s]
A	State space state matrix	
B	State space input matrix	
B_d	State space disturbance matrix	
C	State space output matrix	
x	State vector	
u	State space input vector	
u_d	State space disturbance vector	

Two models for describing the liquid system on the test rig were presented in this chapter, a nonlinear and a linear model. Both models will be considered in the next chapter where the MPC will be developed.

Controller design 5

This chapter will describe the design and use of the model predictive controllers which will be used to control the liquid system. Two controllers are considered in this chapter: A nonlinear model predictive controller, and a linear model predictive controller. Both MPCs will use the models described in chapter 4. The nonlinear model predictive control (MPC) will use the nonlinear model, and the linear MPC will use the linearized model. In the end of the chapter, the two controllers will be compared when controlling a simulated plant.

5.1 Nonlinear MPC

The nonlinear MPC will calculate the control signal for the regulator valve based on the nonlinear model found. This controller will use the nonlinear MPC from MATLAB's Model Predictive Control Toolbox. Figure 5.1 illustrates the control loop for the MPC.

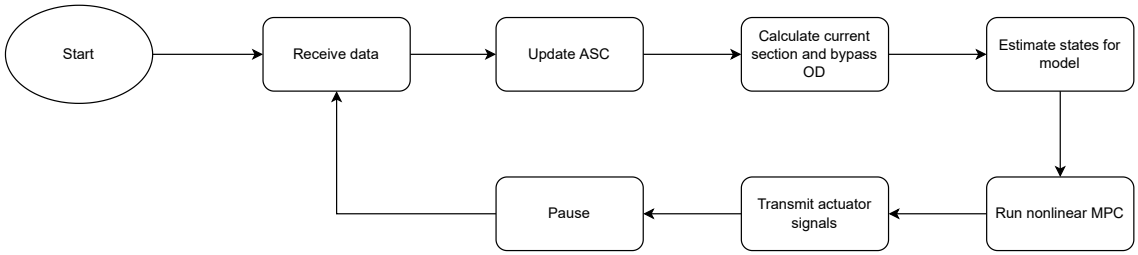

Figure 5.1. Control loop for the nonlinear MPC.

5.1.1 State estimator

A Kalman filter is used to estimate the four states in the nonlinear model. Specifically due to the nonlinear model, an unscented kalman filter (UKF) is used. Two of the states, the boom pressure and the regulator valve angel, are measured directly. For the sake of convenience, the values for the states θ_{bp} and θ_{sec}, are found through open loop simulations performed online when the controller is running. Thus, the purpose of the filter is merely to remove noise, as the value of all states are either measured or obtained otherwise. For the state estimator the discrete time model in equation 5.1 is assumed, where w is the noise on the states, and v is the noise on the output.

$$\begin{aligned} x(k+1) &= F(x(k), u(k)) + w(k) \qquad w \in \mathrm{N}(0, Q_n) \\ y(k) &= G(x(k), u(k)) + v(k) \qquad v \in \mathrm{N}(0, R_n) \end{aligned} \tag{5.1}$$

y	Measured plant output
F	Discrete time state space function
G	Discrete time state space output function
w	Model state noise
Q_n	State noise covariance
v	Model output noise
R_n	Model output noise covariance

The nonlinear model from chapter 4 is discretized in time using a forward euler approximation, thus the model is given by equation 5.2.

$$\begin{aligned} x(k+1) &= x(k) + f(x(k), u(k))\, t_s \\ y(k) &= g(x(k), u(k)) \end{aligned} \tag{5.2}$$

f	Continuous time state space function	
g	Continuous time state space output function	
t_s	State estimator sampling time	[s]

The UKF works in two stages: The measurement update and the time update [7]. In the measurement update, the current estimate for the state vector is calculated, based on both the measured and predicted output of the system, y and $\hat{y}$ respectively, as well as the kalman gain, K, and the state error covariance, P. In the time update stage, the state variables are propagated one time step into the future, $\hat{x}_{k-1}$, as well as the state error covariance, P_{k-1}. The predicted output is found using the output function and the predicted states, thus an initial guess for the states are required for the filter. The steps involved with the measurement and time update steps are shown below. Unlike the linear kalman filter, the covariances, and expected values are found by sampling the state and output function at specific points, determined via the unscented transform.

Measurement update

1. Calculate expected value of $\hat{y}$, the covariance between $\hat{y}$ and $\hat{x}_{k-1}$, and the covariance of $\hat{y}$ via the unscented transform
2. Calculate the covariance of the output error
3. Find error between expected output and actual output
4. Calculate the kalman gain
5. Find current state estimate
6. Calculate state error variance

Time update

1. Calculate the expected value of the predicted state at the next time sample
2. Calculate the predicted state error variance

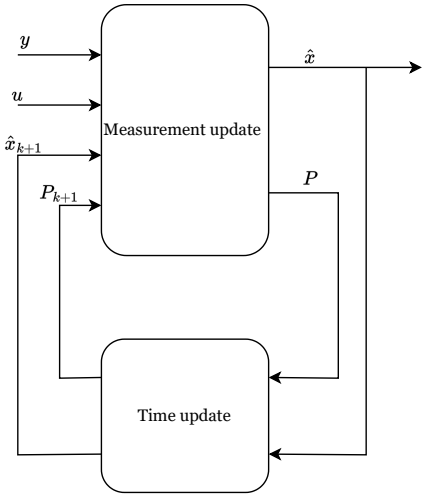

Figure 5.2. Illustration of data flow in the UKF.

The unscented transform is given as function of the model output function, predicted states, inputs, and the predicted state error covariance. The output of the function is the predicted output, its covariance, and the covariance between the predicted output error, and the predicted state error. The predicted output is found by taking the mean of several outputs, generated by evaluating the output function at several test points. The test points are found perturbing the predicted state vector $\hat{x}_{k-1}$. From the perturbed states and the predicted outputs, the two covariances are estimated.

$$\begin{bmatrix} \hat{y}_k \\ \text{Cov}(\tilde{y}_{k-1}, \tilde{x}_{k-1}) \\ \text{Cov}(\hat{y}) \end{bmatrix} = U(g, \hat{x}_{k-1}, u(k), P_{k-1}) \tag{5.3}$$

$\hat{y}$	Predicted output of plant from previous time update
$\tilde{y}_{k-1}$	Predicted output error
$\tilde{x}_{k-1}$	Predicted state error
$\hat{x}_{k-1}$	Predicted state space vector from previous time update
P_{k-1}	Predicted state error covariance from previous time update

For step 2 of the measurement update, the output error covariance is found via equation 5.4.

$$\text{Cov}(\tilde{y}) = \text{Cov}(\hat{y}) + R_n \tag{5.4}$$

The simplest step in running the UKF is finding the output error in the measurement update. The step is given by equation 5.5.

$$\tilde{y} = y - \hat{y} \tag{5.5}$$

The kalman gain is used to correct the predicted states, according to the measured output. The kalman gain is given by equation 5.6.

$$K = \text{Cov}(\tilde{y}_{k-1}, \tilde{x}_{k-1})^T \text{Cov}(\tilde{y})^T \tag{5.6}$$

K	Kalman gain

The current state estimate is given by the correcting the predicted state with the kalman gain and the output error, as done in equation 5.7.

$$\hat{x} = \hat{x}_{k-1} + K\tilde{y} \tag{5.7}$$

$\hat{x}$	Estimated state vector

As the final step of the measurement update, the current state error covariance is found using equation 5.8.

$$P = P_{k-1} - K\text{Cov}(\tilde{y}_{k-1}, \tilde{x}_{k-1}) \tag{5.8}$$

P	State error covariance

The time update will predict the states at the next time sample, x_{k+1} using the unscented transform, and the predicted state error covariance. Both of the predictions will be used the next time the measurement update is performed. The unscented transform will in this case use the discrete time state function, f, with the currently estimated state, $\hat{x}$, and the current state error covariance P.

$$\begin{bmatrix} \hat{x}_{k+1} \\ \text{Cov}(\hat{x}) \end{bmatrix} = U(f, \hat{x}, u(k), P) \tag{5.9}$$

The second and final step in the time update is the predicted state error covariance, P_{k+1}, which is found by equation 5.10.

$$P_{k+1} = \text{Cov}(\hat{x}) + Q_n \tag{5.10}$$

5.1.2 Controller

An MPC generates a control signal based upon a prediction of the plants future behavior based on its current state and what disturbances are to be expected. The control signal is found by minimizing an associated cost function describing the plant's deviation from some reference, and how much the control signal changes. The prediction is done using a model of the plant, in this case it is the nonlinear model derived in chapter 4. The MPC is not capable of predicting an infinitely long time into the future, but only a limited amount of time samples, the prediction horizon, N_p. The MPC does not have to generate a control signal for all time samples it predicts, it only generate signals until the control horizon N_c. The control horizon is usually shorter than the prediction horizon, in order to reduce the amount of variables it has to optimize over. Additionally, with a longer prediction horizon than control horizon, it is capable of finding a set of control signals which stabilizes the plant.

As the nonlinear model does not guarantee a convex problem, the nonlinear MPC will have to optimize a more complex problem than if it was convex. For the nonlinear MPC there is also the chance that it will reach a local minimum which will not result in the most optimal way to actuate the plant, but which the MPC will be trapped in. The result of the optimization is based on the initial conditions, the current state estimate, the previous control signal, and the initial set of future controls. The MPC used in this chapter is the nonlinear MPC provided by Mathworks Model Predictive Control Toolbox, utilizing the non-convex solver FMINCON.

As the MPC is an optimizing controller, it is possible to implement constraints on the output and input, which the controller will consider when generating the control signal. To ensure that the optimization can complete if the current output is beyond the feasible region for the optimization problem, a slack variable, ε is added to these constraints. The slack variable increases the cost of a solution drastically if the output of the plant moves

beyond the constraints [8]. An example of an output constraint is given in equation 5.11, where the maximum output is given by y_{max}.

$$y(i) - \varepsilon \leq y_{max} \tag{5.11}$$

ε	Model Predictive Controller slack variable	[]
y_{max}	Model Predictive Controller maximum output constraint	[]

The cost function for the MPC determines how the set of control signals generated will look, the MPC will find the set of future inputs which minimizes the value of the cost function. The cost function consists of three terms: A reference tracking term, an input rate term, and a slack variable cost term. The reference tracking term provides a cost dependent on the system outputs distance from the reference for that output, the greater the distance, the greater the cost. The input rate term increases the cost for changing the value of the control signal, thus punishing the controller from making very large changes in small amounts of time, and oscillation the control signal. The slack variable term is included in order for the cost function to increase when the constraints are violated, without the term the controller would not even consider the slack variable. For a single output single controlled output system, as the one from chapter 4, the cost function is given by equation 5.12. The cost function is quadratic such that no matter whether the reference error is positive or negative, it is punished, as well as punishing both positive and negative changes of the control signal. Both terms are scaled using a constant values, q for the reference error, and s for the input rate term.

$$J = \sum_{i=1}^{N_p} q \ (r(i) - y(i))^2 + \sum_{i=1}^{N_c} s \ (u(i) - u(i-1))^2 + \sum_{i=1}^{N_p} v \ \varepsilon(i)^2 \tag{5.12}$$

J	Model Predictive Controller cost function	[]
N_p	Model Predictive Controller prediction horizon	[]
N_c	Model Predictive Controller control horizon	[]
q	Reference deviation cost multiplier	[]
r	Setpoint reference for Model Predictive Controller	[]
s	Control signal rate of change cost multiplier	[]
v	Slack variable cost multiplier	[]

5.1.3 Controller validation

The state estimator and the nonlinear MPC will be validated by simulating a run of the spray map from chapter 2. From the plots in figure 5.3, the UKF is tested on a step

response of the section valves. The filter fulfills its purpose of filtering out measurement noise.

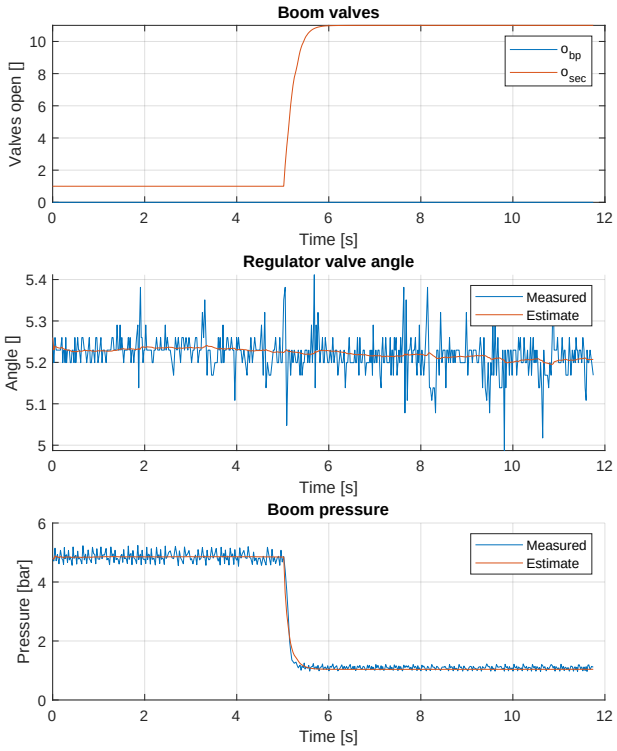

Figure 5.3. Test of the UKF on measured data.

The MPC has been tuned, such that the controller uses the parameters given in table 5.1. The prediction horizon is chosen to be long enough for the controller to acknowledge that the amount of open sections will change some time in advance, but short enough for the controller to not have a very long execution time.

Parameter	N_p	N_c	t_s	q	s
Value	10	5	0.10 s	10	0

Table 5.1. Tuned parameters used by the nonlinear MPC.

From the resulting states of the simulation run in figure 5.4, it is confirmed that the pressure settling time is fulfilled on stretch A, and at the point where the application rate setpoint changes. Requirement A limiting the pressure to at max 8.0 bar is also fulfilled.

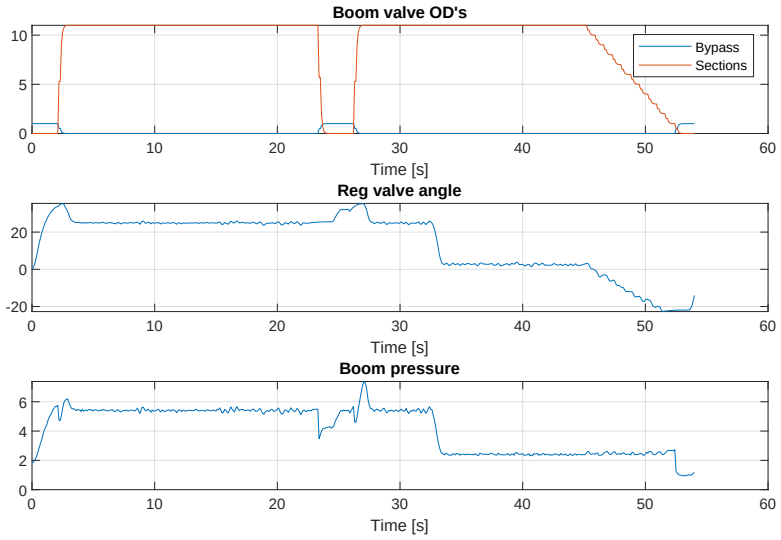

Figure 5.4. States from simulation of the nonlinear MPC.

The requirement for the maximum deviation of the application rate while at steady state, is fulfilled by this controller, as shown in figure 5.5b.

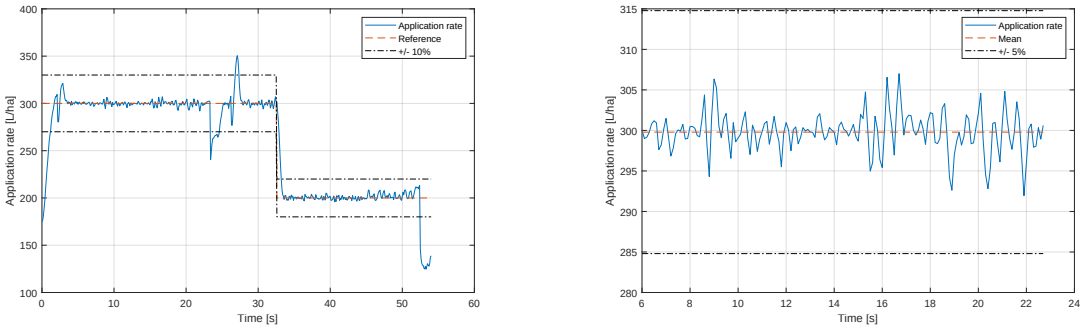

(a) Entire run. ***(b)*** stretch A.

Figure 5.5. Application rate during the validation test.

An issue with this controller is the execution time for each run through the control loop, plotted in figure 5.6. The mean execution time is 5.3 s, which is significantly longer than the time constants for both the regulator valve and section valves. At a speed of 20.0 km h^{-1} the sprayer would have covered a distance of 30.0 m between each update cycle.

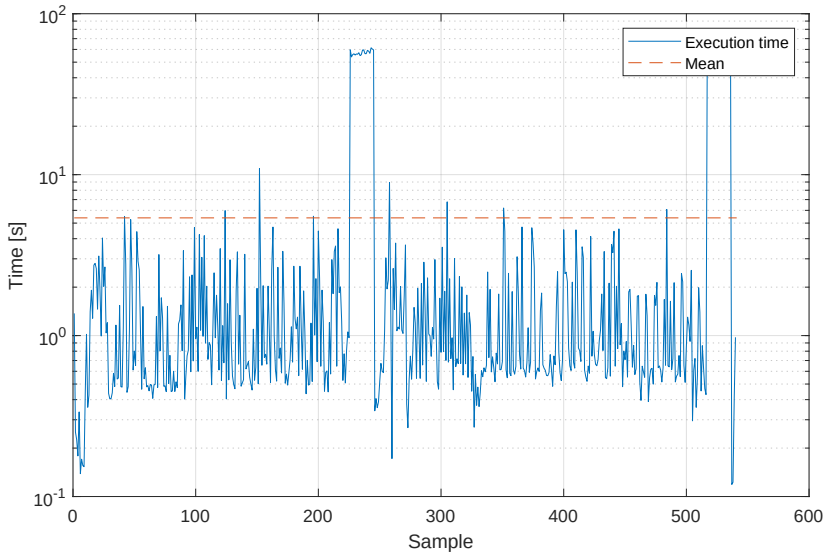

Figure 5.6. Execution time of the nonlinear MPC.

5.2 Linear MPC

A nonlinear MPC is not needed when a linear model is provided, and the constraints are linear. In that case it is possible to setup a convex optimization problem for the MPC, which can significantly decrease its execution time. In this section, the linear model from section 4.2 will be used for such an MPC, in order to decrease the execution time of the controller from section 5.1.

For this controller the prediction of the restrictions on the boom, r_{bp}, r_{sec}, and their change over time, $\dot{r}_{bp}$, $\dot{r}_{sec}$, are not done by the MPC, but are instead calculated before hand, being used as time varying gains and measured disturbances respectively.

The two states in the linear model, p_b and G_R, are found via the UKF, using the nonlinear model, described in section 5.1.1. p_b are taking directly as one of the estimated states, while the gain is found using the estimated restrictions, r_{bp} and r_{sec}, as well as the estimated regulator valve angle, using the definition of G_R from equation 4.9.

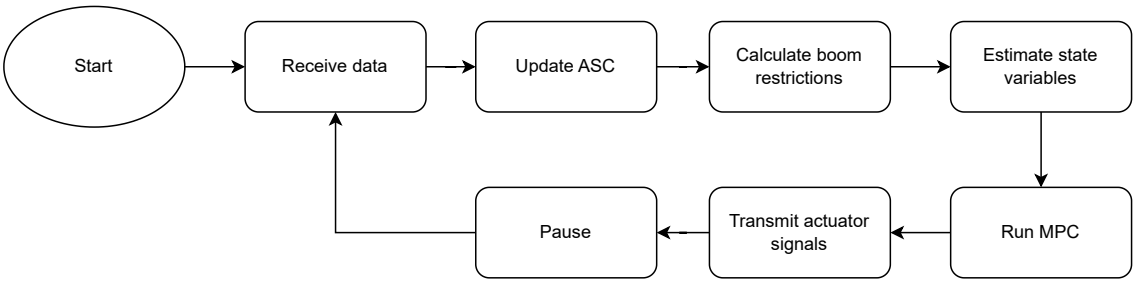

Figure 5.7. Update loop for the linear MPC.

5.2.1 Controller

The linear MPC developed for this project is based on the MPC described by Wang [9]. The MPC uses a set of lifted system matrices to calculate the predicted output and uses this to generate the control signal.

In order for the controller to implement integral action, an augmented discrete time plant model is used. The plant is discretized using a forward euler approximation. The augmented model incorporates the controlled output of the plant, as well as the change in the states and inputs from one time sample to the next, as illustrated in equation 5.13.

$$\begin{aligned} \begin{bmatrix} \Delta x(k+1) \\ y(k+1) \end{bmatrix} &= A_a \begin{bmatrix} \Delta x(k) \\ y(k) \end{bmatrix} + B_a \Delta u + B_{d,a} \Delta u_d \\ y(k) &= C_a \begin{bmatrix} \Delta x(k) \\ y(k) \end{bmatrix} \end{aligned} \tag{5.13}$$

The augmented state space matrices are given by equation 5.14.

$$\begin{aligned} A_a &= \begin{bmatrix} A & 0 \\ C\ A & I \end{bmatrix} & B_a &= \begin{bmatrix} B \\ C\ B \end{bmatrix} \\ B_{d,a} &= \begin{bmatrix} B_d \\ C\ B_d \end{bmatrix} & C_a &= \begin{bmatrix} 0 & I \end{bmatrix} \end{aligned} \tag{5.14}$$

The future response of the system can be found by continuously evaluating the discrete time system, as done in equation 5.15.

$$\begin{aligned} x_a(k+1) =& A_a x_a(k) + B_a \Delta u(k) + B_{d,a} \Delta u_d(k) \\ x_a(k+2) =& A_a x_a(k+1) + B_a \Delta u(k+1) + B_{d,a} \Delta u_d(k+1) \\ =& A_a \left(A_a x_a(k) + B_a \Delta u(k) + B_{d,a} \Delta u_d(k) \right) + B_a \Delta u(k+1) + B_{d,a} \Delta u_d(k+1) \\ =& A_a^2 x_a(k) + A_a\ B_a\ \Delta u(k) + B_a\ \Delta u(k+1) + A_a\ B_{d,a}\ \Delta u_d(k) + B_{d,a} \Delta u_d(k+1) \\ & \dots \end{aligned} \tag{5.15}$$

The output of the system can be found from the prediction model above by left multiplying with the augmented output matrix C_a.

$$\begin{aligned} y(k+1) &= C_a\ A_a x_a(k) + C_a\ B_a \Delta u(k) + C_a\ B_{d,a} \Delta u_d(k) \\ y(k+2) &= C_a\ A_a^2 x_a(k) + C_a\ A_a\ B_a\ \Delta u(k) + C_a\ B_a\ \Delta u(k+1) \\ &\quad + C_a\ A_a\ B_{d,a}\ \Delta u_d(k) + C_a\ B_{d,a} \Delta u_d(k+1) \\ &\dots \end{aligned} \tag{5.16}$$

Equation 5.16 can be rewritten into a sum of matrix vector products, as done in equation 5.17. The future input change vector $\Delta\mathcal{U}$ is the optimization variable in this prediction system. The state vector $x_a(k)$ and future disturbance input $\Delta\mathcal{U}_d$ are known in advance, from the state estimator and the auto section controller (ASC) respectively.

$$\begin{aligned} \begin{bmatrix} y(k+1) \\ y(k+2) \\ \dots \end{bmatrix} &= \begin{bmatrix} C_a\ A_a \\ C_a\ A_a^2 \\ \dots \end{bmatrix} x_a(k) + \begin{bmatrix} C_a\ B_a & 0 & \dots \\ C_a\ A_a\ B_a & C_a\ B_a & \dots \\ \vdots & \vdots & \vdots \end{bmatrix} \begin{bmatrix} \Delta u(k) \\ \Delta u(k+1) \\ \vdots \end{bmatrix} \\ &\quad + \begin{bmatrix} C_a\ B_{d,a} & 0 & \dots \\ C_a\ A_a\ B_{d,a} & C_a\ B_{d,a} & \dots \\ \vdots & \vdots & \vdots \end{bmatrix} \begin{bmatrix} \Delta u_d(k) \\ \Delta u_d(k+1) \\ \vdots \end{bmatrix} \\ \longrightarrow \mathcal{Y} &= \mathcal{F} x_a(k) + L\Delta\mathcal{U} + M\Delta\mathcal{U}_d \end{aligned} \tag{5.17}$$

For the linear model MPC in this report, only an input constraint is used. The input constraint is present to limit the gain G_R between 0 and 1. The input constraint is given by equation 5.18, integrating the control signal using the optimization variable.

$$G_{R,min} \leq u(k-1) + \begin{bmatrix} 1 & 0 & 0 & \dots \\ 1 & 1 & 0 & \dots \\ \vdots & & & \end{bmatrix} \Delta\mathcal{U} \leq G_{R,max} \tag{5.18}$$

For this MPC, the cost function is similar to the one in equation 5.12 from the nonlinear MPC. Though the slack variable term is excluded as there is no output constraint implemented.

$$J = \sum_{i=1}^{N_p} q\ \left(r(i) - y(i)\right)^2 + \sum_{i=1}^{N_c} s\ \Delta u(i)^2 \tag{5.19}$$

5.2.2 Controller validation

The controller is tested on the spray map described in chapter 2, with the simulation plant using the nonlinear model described from chapter 4. Using the simulations, the controller has been tuned to use the parameters listed in table 5.2 for its validation run.

Parameter	N_p	N_c	t_s	q	s
Value	40	20	200.0E−3 s	20	20

Table 5.2. Tuned parameters used by the linear MPC.

An animation of the validation run can be found via the link below.

`https://github.com/soerenLang/mpc4sprayer_public/blob/main/27-May-2024%2009-06-40.gif`

Figure 5.8 shows the resulting pressure and regulator angle. The boom pressure does not exceed the maximum pressure requirement of 8.0 bar, nor the settling time requirement of 7.0 s.

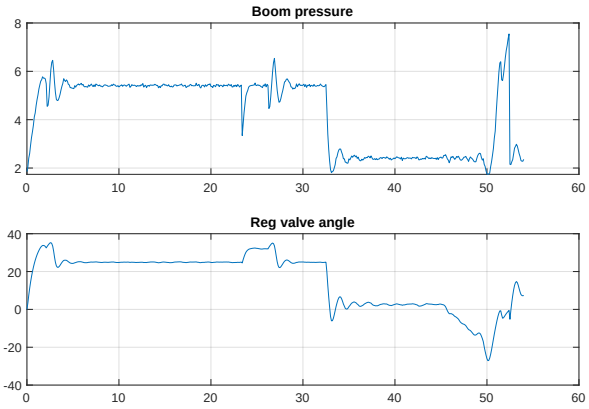

Figure 5.8. Simulation results of the linear MPC running.

The application rate from the validation run, shown in figure 5.9a, fulfills the settling time requirement. Additionally the maximum application rate deviation requirement is also fulfilled, as shown in figure 5.9b.

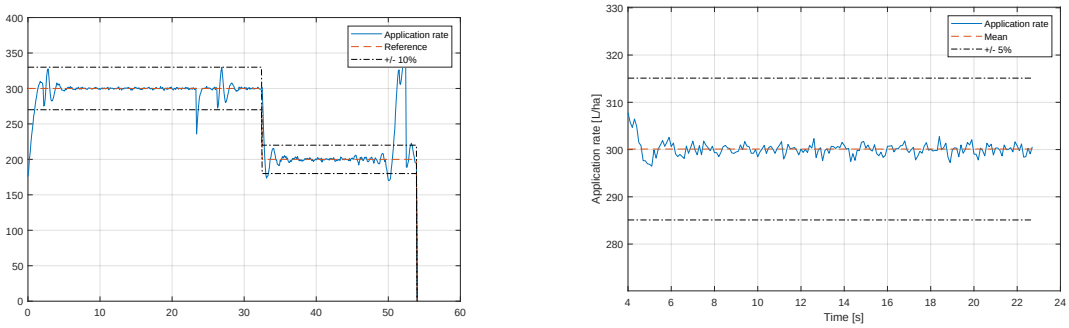

(a) Entire run. *(b)* stretch A.

Figure 5.9. Application rate during the validation test.

Finally, the linear MPC runs significantly faster than the nonlinear MPC, when comparing the execution time per update in figure 5.10, with the execution time from section 5.1.3. The sampling time will be increased though to 200.0 ms in order for the system to be guaranteed a constant loop time.

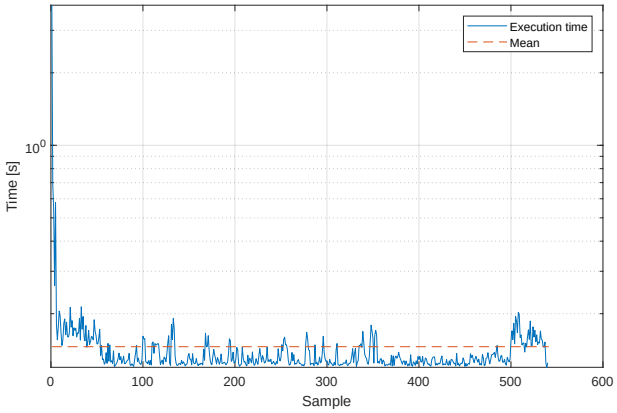

Figure 5.10. Execution time of the linear MPC.

Due to all parts of the validation run fulfilling the requirements, the linear MPC is chosen as the controller used for the acceptance test on the test rig, described in the next chapter.

Acceptance test 6

This chapter will describe the results of the acceptance test. The acceptance test is performed in order to verify that the model predictive controller (MPC) upholds the requirements set forth in chapter 2 when comtrolling the test rig described in chapter 3. The test will be performed using the linear MPC described in section 5.2, with the linear system model found in section 4.2. Figure 6.1 shows the three plots which will be used to analyze the test, an animation of the acceptance run can be found via the link below.

`https://github.com/soerenLang/mpc4sprayer_public/blob/main/17-May-2024%2010-52%20output%20animation.gif`

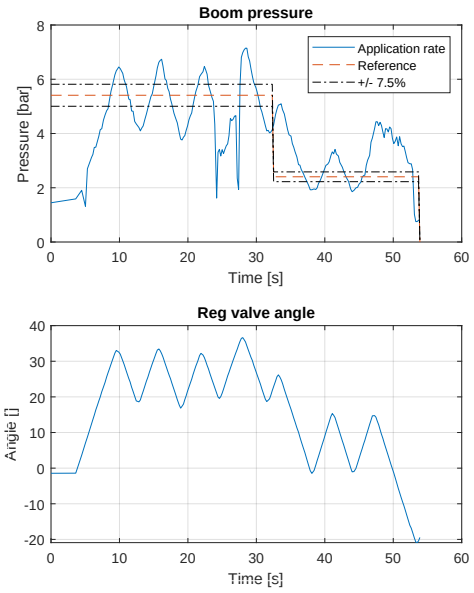

(a) Plant output during acceptance test.

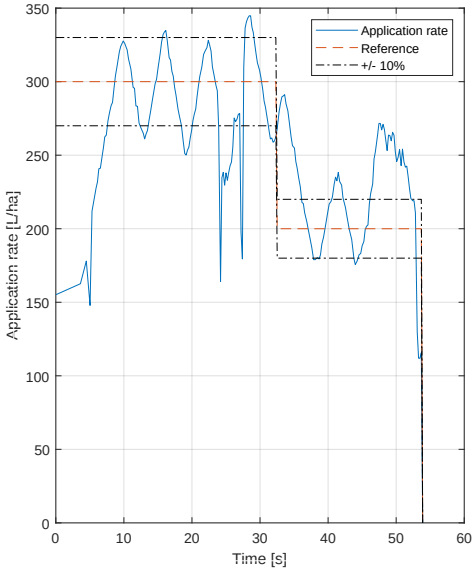

(b) Plant application rate during acceptance test.

Figure 6.1. Plots from acceptance test.

Requirement 1 is fulfilled if the pressure settles to within $\pm 7.5\,\%$ of the setpoint. From figure 6.1 it is seen, that the pressure does not settle, but oscillates, thus the requirement is not fulfilled. As the pressure oscillates, so does the application rate. The application rate oscillates beyond the settling limits, thus never settling, not fulfilling the settling time of requirement 2, and the maximum application rate deviation from requirement 3.

The last requirement, requirement A, is fulfilled. The boom pressure never exceeds the maximum pressure of 8.0 bar during the test.

Requirement	Description	Fulfilled
1	Maximum steady state pressure offset ±7.5 %	✗
2	Application rate settling time less than 7.0 s	✗
3	Max application rate deviation at steady state, 5.0 %	✗
A	Max boom pressure less than 8.0 bar	✓

Table 6.1. Summary of results from acceptance test.

6.1 Discussion of results

The results of the acceptance test differs from the ones obtained by the simulation. Where the simulated controller was capable of fulfilling all the requirements, using the controller on a real life system resulted in only a single requirement being fulfilled. One of the things that could affect the difference is the behaviour of the regulator valve. The relationship between the valve and the gain in the controller, G_R, is nonlinear. Thus, it was not possible to set linear constraints on the rate of change of the gain. Additionally, it was attempted to introduce a time delay into the gain by modelling it as a first order system. Figure 6.2 shows the regulator valve angle and its control signal, the regulator valve on the real system moves significantly slower than in the simulation. A time delay is also observed in the acceptance test when the valve changes direction, this is due to combination of communication delay between the controller and the smartcom electronic control unit (ECU), as well as the mechanical construction of the valve.

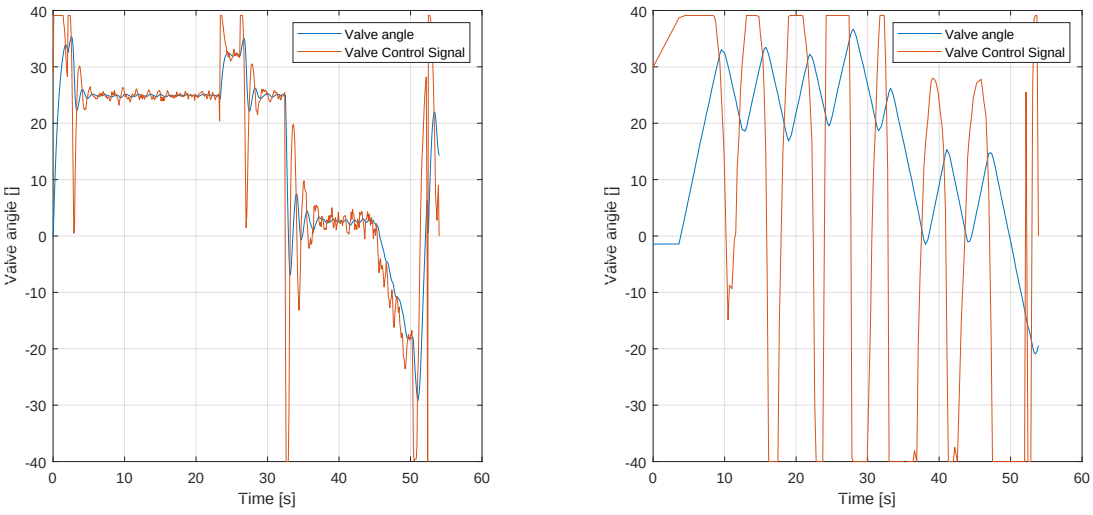

(a) Simulation. ***(b)*** Acceptance test.

Figure 6.2. Comparison between regulator valve control signal and the valve angle.

In early simulations a similar problem to the one in the acceptance test was observed, where the controller employed a bang-bang form of control, this was resolved by lowering the time constant of the gain significantly. The same solution was attempted for this controller early in the test regime, where the time constant was lowered even further, though with little success.

7 Conclusion

Field sprayers are large and complex machines with a specific purpose: To deliver chemicals in the form of herbicides or fertilizers, to plants in a field. A focus of modern sprayers are to spray only where is needed, while providing a more robust and consistent spraying system. Systems which automatically switches sections of the sprayer on or off exists and are based upon Global Navigation Satellite Systems (GNSSs). The switching systems disturbs the liquid system, thus a control scheme is needed in order to keep a constant pressure. It was proposed that a model predictive controller (MPC) would be capable of controlling such a liquid system, specifically using the predictive properties of the controller to anticipate the change in open sections, and thus priming the liquid system for the disturbances.

Controllers for sprayer liquid systems must comply with the ISO 16119-2 standard, as well as the physical constraints the components of the sprayer imposes. For this project, a test rig emulating a field sprayer was created, with all the various components needed for a sprayer to function.

For the model predictive controller, a nonlinear hydraulic model of a liquid system was developed. The model was capable of describing the changing fluid restrictions on the boom from the sections, as well as the change in pressure when turning the systems regulator valve. A linear version of the model was developed as well, which assumed a constant pump flow and precalculated the pressure changes from sections turning on and off. Two types of MPCs was tested, a nonlinear version and a linear version. The nonlinear MPCs was only tested in simulation as the execution time for the controller was well above what was necessary to control the system. The linear MPC was tested on the test rig, as it fulfilled all the requirements in the simulations. The linear controller was only able to fulfill 1 out of 4 requirements when used on the test rig.

8 Discussion

In this chapter, certain areas which required more attention and work, than was possible in the rest of the report is touched upon and discussed.

8.1 Nonlinear MPC

Even though it was decided to not go ahead with the nonlinear model predictive controller (MPC) described in section 5.1 due to the long execution time, there are some techniques which could be used to improve the performance of the controller.

The prediction and control horizon was chosen to be 10 and 5 samples respectively, such that the controller would be able to use the anticipated disturbances, these could be lowered even further, thereby reducing the execution time significantly. If the prediction horizon was lowered to 2 samples and the control horizon lowered to 1 sample, the average execution time would well below 0.50 s.

The execution time could be reduced even further if the model was reduced to a two state model. The controller described in section 5.1 uses the control signals for the bypass and section valves in its prediction, and then calculates the dynamics from those. The controller has to recalculate these several times during the optimization procedure, even though their contribution is exactly the same every time. These calculations could be computed beforehand as done in the control loop for the linear MPC. Removing these from the MPC would also allow for a generalization of the controller, such that little rework would have to be done if it was to be used together with a different liquid system on the boom.

It is also possible to precompile the controller. As MATLAB is an interpreted language, it takes a longer time to run. Having the controller beforehand could reduce the execution time significantly as well.

8.2 Parameter estimation

The MPC requires an accurate model in order to function properly, the more precise the model, the better prediction, the more optimal control. The liquid system of the sprayer is significantly more complex than what the test rig represents, with several filters placed throughout the system, filters which can be clogged and reduce the likeness between the

model and the system. To achieve a more representative model, the parameters in the system could be estimated. For the nonlinear model there are essentially four parameters, which needs to be estimated: R_{bp}, R_{sec}, R_B, and R_r. If the pump flow is assumed constant, the pump restriction R_p, does not need to be estimated, as the only relevant thing for the model would be the flow into the regulator valve boom junction. The two dynamic boom restrictions can be estimated with the current set of sensors, the boom pressure sensor and the boom flow sensor. In order to estimate R_B and R_r, another set of flow and pressure sensors would be needed. The pressure sensor should be placed at the junction where the regulator valve diverts the pump flow away from the boom, while the flow sensor should be placed in order to measure the pump flow. The flow sensors accuracy increases as the flow increases, thus it should be placed where the largest flow is present, which is out of the pump. The resulting piping and instrumentation diagram is shown in figure 8.1. R_B and R_r can be described by equation 8.1.

$$\begin{aligned} R_B &= \frac{p_r - p_b}{Q_b^2} \\ R_r &= \frac{p_r}{(Q_p - Q_b)^2} \end{aligned} \tag{8.1}$$

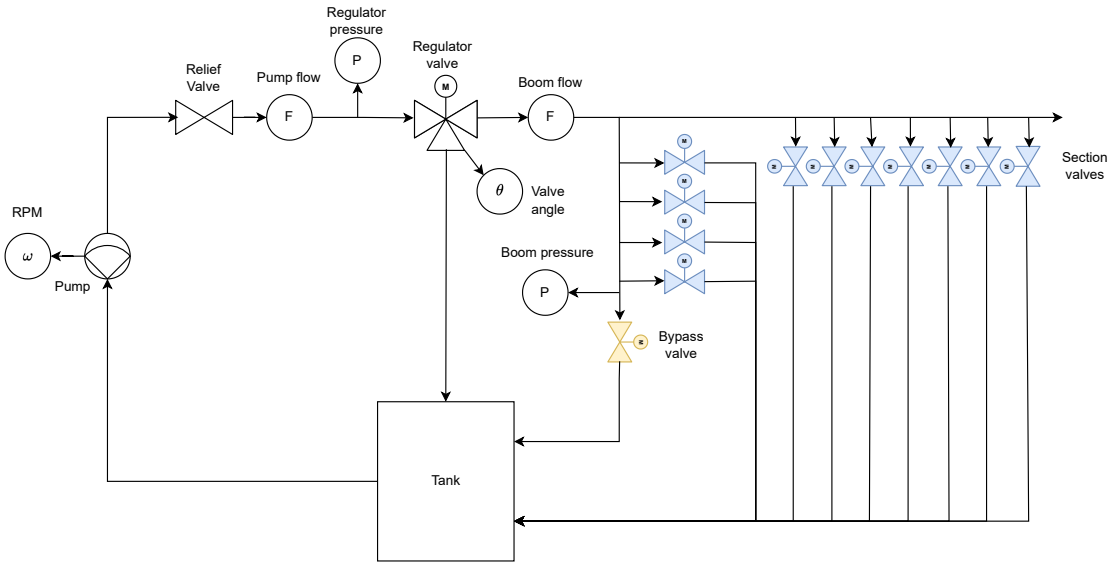

Figure 8.1. Piping and instrumentation diagram for the system if parameter estimation should be implemented.

The function describing R_r could be found by doing online least squares fitting, in the same manner as done in appendix A.

8.3 Alternative liquid system

Throughout this report the rotational velocity of the pump was considered constant, as sprayers have no control of the tractors power take-off (PTO). But if the pump was con-

trollable by the sprayer, if it was driven by a high pressure hydraulic system for instance, it would be possible to remove the regulator valve entirely from the system. Such a system is illustrated in figure 8.2, where the pumps rotational speed is controlled by a proportional hydraulic valve. The simplification would remove a lot of complexity from the interconnected liquid system, and separate the control problem into two systems, a hydraulic and a liquid system, which could have the potential to be modelled independently of each other. If a parameter estimator was implemented, fewer sensors would be required, as there are fewer nodes in the system.

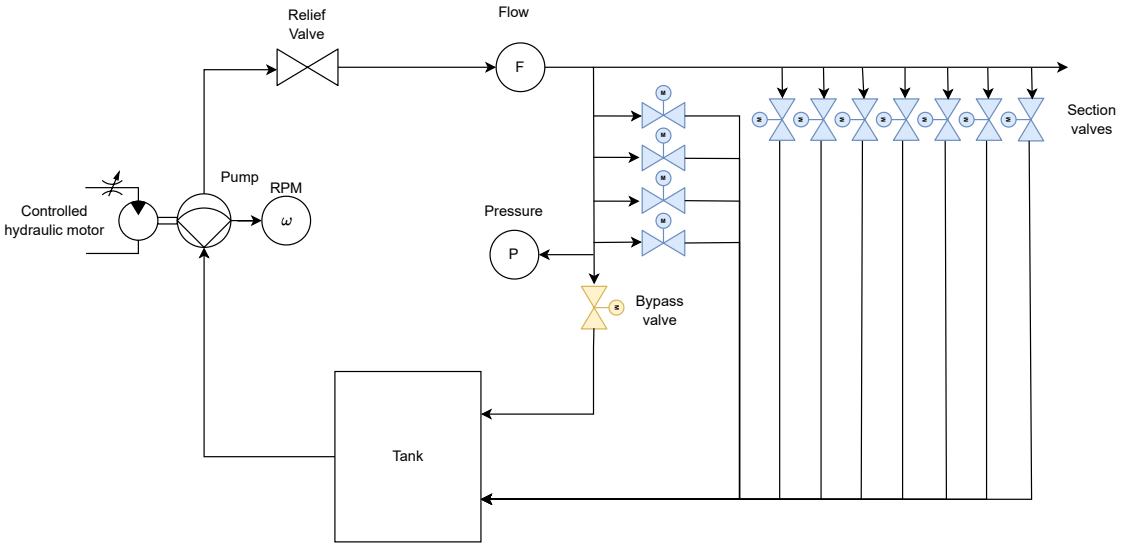

Figure 8.2. Alternative to the liquid system used in the thesis.

Bibliography

[1] Adrees Khan et al. "Design and Implementation of Model Predictive Control (MPC) Based Pressure Regulation System for a Precision Agricultural Sprayer". eng. In: *2023 International Conference on Robotics and Automation in Industry (ICRAI)*. IEEE, 2023, pp. 1–6. ISBN: 1665464720.

[2] Deniver R. Schutz et al. "Advanced embedded generalized predictive controller based on fuzzy gain scheduling for agricultural sprayers with dead zone nonlinearities". In: *Journal of Process Control* 135 (2024), p. 103164. ISSN: 0959-1524. DOI: https://doi.org/10.1016/j.jprocont.2024.103164. URL: https://www.sciencedirect.com/science/article/pii/S0959152424000040.

[3] Kleber R. Felizardo et al. "Modeling and Predictive Control of a Variable-Rate Spraying System". In: *2013 8th EUROSIM Congress on Modelling and Simulation*. 2013, pp. 202–207. DOI: 10.1109/EUROSIM.2013.46.

[4] *Agricultural and forestry machinery - Environmental requirements for sprayers - Part 2: Horizontal boom sprayers*. Standard. Kollegievej 26, DK-2920 Charlottenlund: Dansk Standard, Mar. 2013.

[5] C. De Persis and C. S. Kallesoe. "Pressure Regulation in Nonlinear Hydraulic Networks by Positive and Quantized Controls". eng. In: *IEEE transactions on control systems technology* 19.6 (2011), pp. 1371–1383. ISSN: 1063-6536.

[6] Olav Egeland and Jan Tommy Gravdahl. *Modeling and Simulation for Automatic Control*. Corr. 2. printing. Trondheim: Marine Cybernetics, 2002. ISBN: 8292356010.

[7] Mohinder S Grewal and Angus P Andrews. *Kalman Filtering: Theory and Practice with MATLAB*. eng. 4th ed. Wiley - IEEE. Somerset: Wiley, 2014. ISBN: 9781118851210.

[8] Francesco Borrelli, Alberto Bemporad, and Manfred Morari. *Predictive Control for Linear and Hybrid Systems*. Cambridge University Press, 2017. ISBN: 978-1-107-65287-3. DOI: 10.1017/9781139061759.

[9] Liuping. Wang. *Model Predictive Control System Design and Implementation Using MATLAB*. eng. 1st ed. 2009. Advances in Industrial Control. London: Springer London, 2009. ISBN: 1-282-01831-0.

Modelling of regulator valve

This appendix will describe the develpoment of a contionous model, describing the regulator valve restriction based upon the regulator valve angle. Based upon measurements of the hydraulic equivalent admittance value for the regulator valve, the linear denominator model and the quadratic denominator model in equations A.1 and A.2 respectively, are proposed.

$$R_{reg}\left(\theta_{reg}\right) = \frac{1}{\left(a\ \theta_{reg} + b\right)} \tag{A.1}$$

$$R_{reg}\left(\theta_{reg}\right) = \frac{1}{\left(a\ \theta_{reg}^2 + b\ \theta_{reg} + c\right)} \tag{A.2}$$

Based upon the fitted models, shown in figure A.1, the quadratic approximation is chosen, as the pole of the model is placed significantly higher valve angle than the the pole of the linear model.

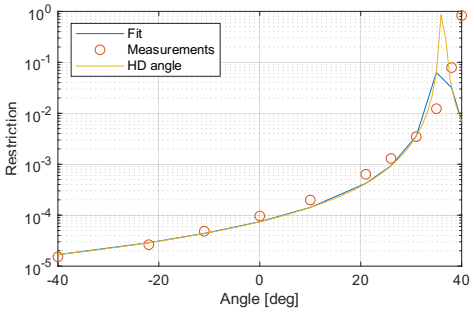

(a) Linear approximation for denominator.

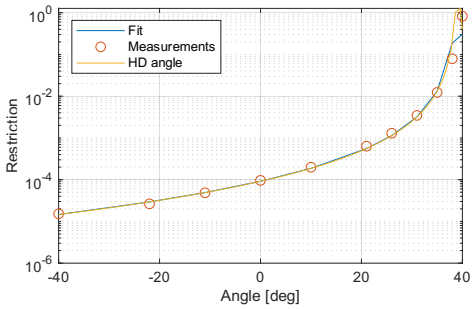

(b) Quadratic approximation for denominator.

Figure A.1. Fitted regulator valve model.

Modelling of bypass valve B

In this appendix a model describing the restriction of the bypass valve as a function of the opening degree, will be found. For an opening degree of 0, the valve restriction should tend towards infinity, such that no or very little liquid passes through. For an opening degree of one, the restriction should tend towards a certain value, thus, the proposed model for the bypass valve is given by equation B.1.

$$R_{bp}(\theta_{bp}) = \frac{G_b p}{\theta_{bp}} \tag{B.1}$$

The gain G_{bp} is found by finding the steady state restriction of the boom while the bypass restriction is open, and all the section valves are closed. The gain is thus found by taking the mean of the three measured restrictions in figure B.1, resulting in $G_{bp} = 67.8\text{E}{-6}$.

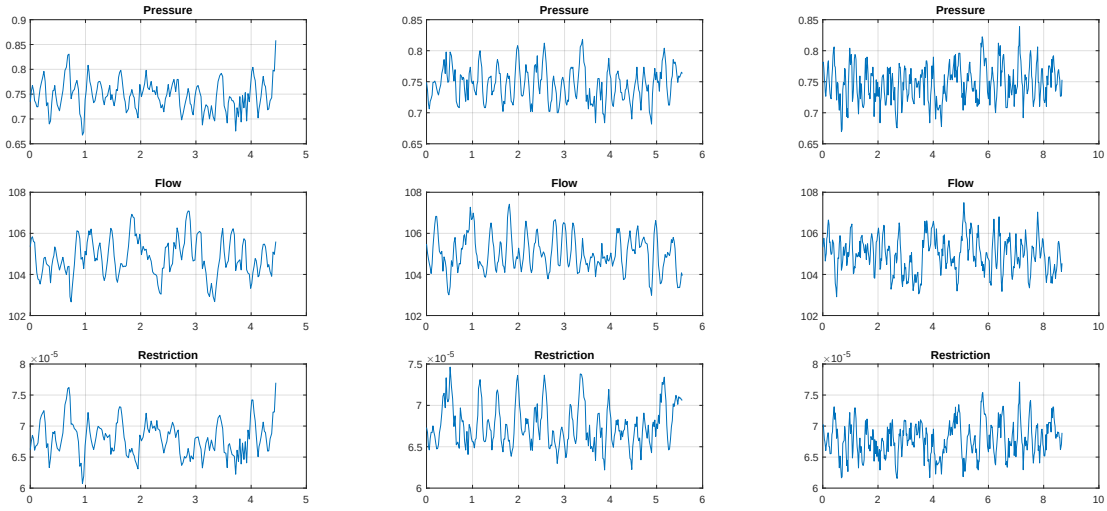

(a) Test 1. ***(b)*** Test 2. ***(c)*** Test 3.

Figure B.1. Plots of the tests used to find the gain G_{bp}.

Modelling of section valves

C

This appendix will describe how the model for the section valves were derived. There are two main things related to the model: The steady state gain, and the dynamics.

C.1 Steady state gain

The steady state gain of the section valves have been found by running the system at different operating conditions, with a different amount of section valves open. The system has been allowed to settle, at which points the pressure and flow to the boom has been measured for some time. The test has been repeated for some number of open section valves. Based on the pressure and the flow, the restriction value has been calculated from the mean flow and pressure of the test using equation C.1. The measured restrictions are given in table C.1

$$R = \frac{p}{Q^2} \tag{C.1}$$

Open valves	1	3	5	6	8	10	11
Test 1	11.8E−3	1.9E−3	667.0E−6	403.0E−6	217.0E−6	126.0E−6	103.0E−6
Test 2	11.7E−3	2.1E−3	653.0E−6	406.0E−6	-	-	101.0E−6
Test 3	11.4E−3	2.2E−3	658.0E−6	389.0E−6	-	-	101.0E−6
Test 4	11.8E−3	2.2E−3	681.0E−6	389.0E−6	-	-	103.0E−6
Test 5	11.8E−3	2.1E−3	667.0E−6	403.0E−6	-	-	100.0E−6
Test 6	11.1E−3	1.9E−3	667.0E−6	403.0E−6	-	-	101.0E−6
Test 7	12.2E−3	-	639.0E−6	-	-	-	103.0E−6
Test 8	11.7E−3	-	694.0E−6	-	-	-	103.0E−6
Test 9	11.4E−3	-	667.0E−6	-	-	-	103.0E−6
Test 10	11.7E−3	-	667.0E−6	-	-	-	100.0E−6
Test 11	10.4E−3	-	683.0E−6	-	-	-	100.0E−6
Mean	11.5E−3	2.1E−3	667.0E−6	399.0E−6	217.0E−6	126.0E−6	102.0E−6

Table C.1. Caption

Based upon the equation for parallel restrictions, the data is attempted fitted to the two functions given in equation C.2. With the results shown figure C.1. The affine power approximation has a mean squared error of 67.7E−9 while the power approximation has a mean squared error of 93.2E−9. Even though the power approximation has the highest mean squared error, it is chosen as the model for the system, due to the better fit at low restrictions.

$$\begin{aligned} R_{sec,1}(\theta_{sec}) &= \frac{a}{\theta_{sec}^2} + b \\ R_{sec,2}(\theta_{sec}) &= \frac{a}{\theta_{sec}^2} \end{aligned} \tag{C.2}$$

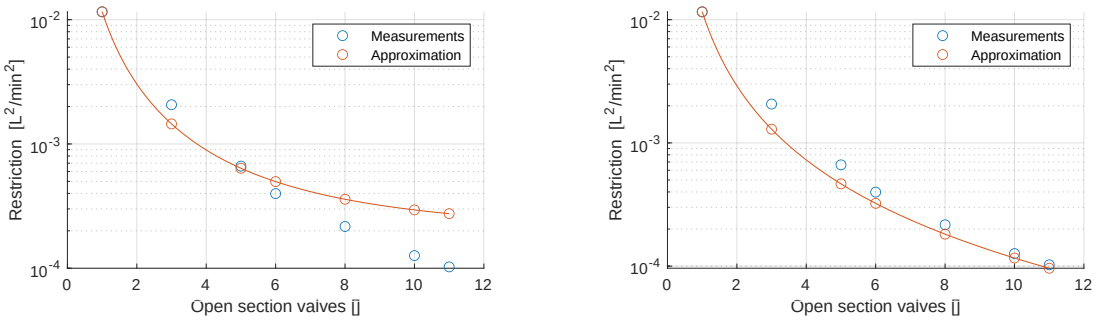

(a) Affine power approximation. *(b)* Power approximation.

Figure C.1. Fitted steady state model for the section valves.

C.2 Dynamics

The dynamical model of the section valves begins by looking at the plots in figure C.2, and realising that the restriction changes like a first order system. It is therefore desired to set up a model which describes the number of open section valves as a first order system.

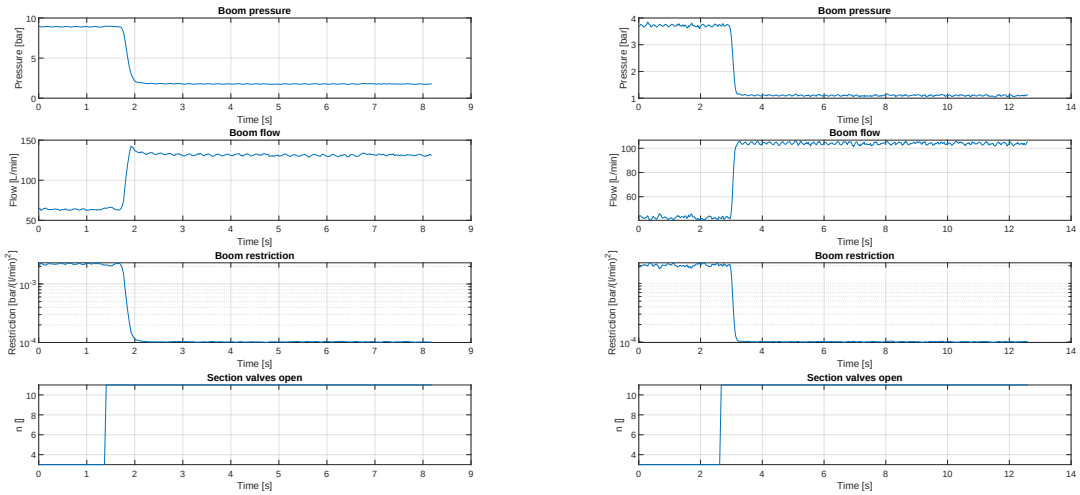

(a) Affine power approximation. *(b)* Power approximation.

Figure C.2. Fitted steady state model for the section valves.

The only variable needed to fit a first order model with a steady state gain of 1, is the time constant. The time constant for several section valve steps are found in table C.2. The time constant is found by finding the mean of the time constants resulting in a time constant for the section valve of 0.2 s.

Test	Start pressure	End pressure	60 % pressure change	Step start time	60 % time	τ
1	1.0 bar	4.0 bar	2.8 bar	2.40 s	2.56 s	0.16 s
2	0.6 bar	1.8 bar	1.3 bar	3.63 s	3.75 s	0.12 s
3	4.8 bar	1.0 bar	2.5 bar	1.44 s	1.56 s	0.12 s
4	7.6 bar	1.3 bar	3.8 bar	3.35 s	3.50 s	0.15 s
5	1.0 bar	4.0 bar	2.8 bar	2.40 s	2.56 s	0.16 s
6	3.8 bar	1.1 bar	2.2 bar	2.94 s	3.07 s	0.13 s
7	8.9 bar	1.7 bar	4.6 bar	1.66 s	1.86 s	0.20 s
8	1.7 bar	8.9 bar	6.0 bar	2.18 s	2.40 s	0.22 s
9	1.3 bar	4.8 bar	3.4 bar	2.27 s	2.49 s	0.22 s
10	0.7 bar	1.9 bar	1.4 bar	1.65 s	1.78 s	0.13 s
11	2.1 bar	4.4 bar	3.5 bar	0.76 s	0.90 s	0.14 s
12	7.2 bar	4.5 bar	5.6 bar	0.60 s	0.74 s	0.14 s
13	2.9 bar	1.8 bar	2.2 bar	0.56 s	0.67 s	0.11 s
14	9.7 bar	5.6 bar	7.2 bar	0.34 s	0.47 s	0.13 s
15	1.8 bar	5.6 bar	4.1 bar	0.26 s	0.44 s	0.18 s

Table C.2. Table for finding the time constant of the section valves.

Modelling of pump D

This appendix will describe the process of acquiring a continuous model describing the pump. The primary source of data is the data in figure D.1. A set of data describing the relationship between pressure, flow and pump revolutions is acquired from the figure.

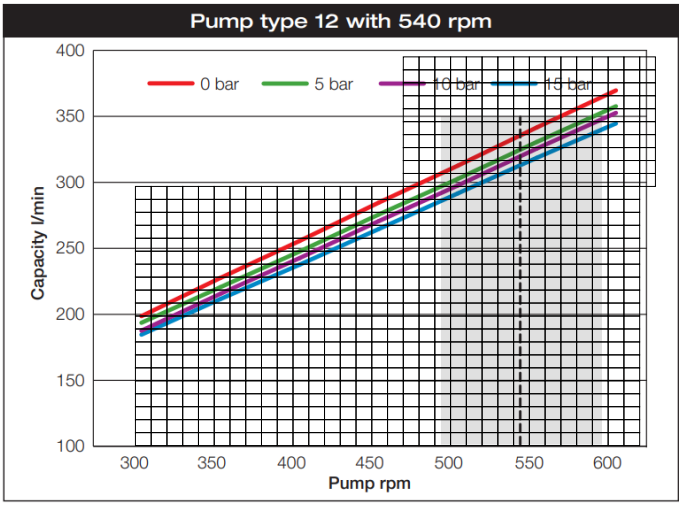

Figure D.1. Flow-RPM-pressure relationship for the pump. [1]

Three models for describing the pressure differential of the pump is fitted to the data: A linear approximation, a quadratic approximation, and a semi quadratic approximation. The three models are given in equations D.1, D.2, and D.3, respectively.

$$\Delta P_p = a\,Q + b\,\omega + c \tag{D.1}$$

$$\Delta P_p = a\,\omega^2 + b\,Q\,\omega + c\,Q^2 + d\,\omega + e\,Q + f \tag{D.2}$$

$$\Delta P_p = a\,Q^2 + b\omega + c\,Q + d + e\,Q\,\omega \tag{D.3}$$

The fitted models are plotted in figure D.2a, along with the fitting data. From the mean squared errors between the model and the data, listed in table D.1, it is seen that the quadratic approximation has the lowest mean squared error (MSE). The semi quadratic model is however chosen as the pump model, due to its finer behaviour in the operating area, not having two possible flow values for a certain amount of revolutions.

[1] Hardi 464 pump datasheet.

Model	Linear	Quadratic	Semi quadratic
MSE	2.8	0.4	1.3

Table D.1. Mean squared error of the three fitted models.

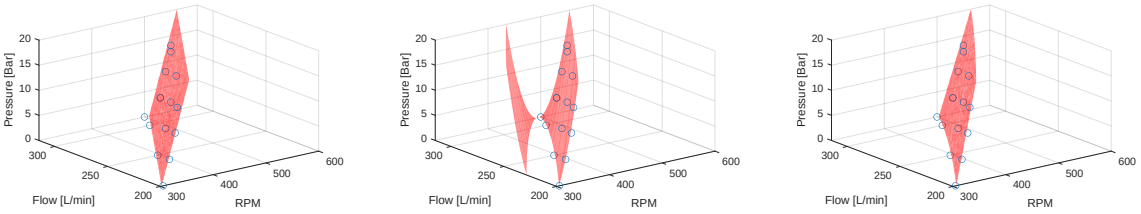

(a) Linear approximation.

(b) Quadratic approximation.

(c) Semi quadratic approximation.

Figure D.2. Plots of the pump models within the expected operating area.